Ore Geology Reviews 34 (2008) 87–112

Contents lists available at ScienceDirect

Ore Geology Reviews

journal homepage: www.elsevier.com/locate/oregeorev

Emerald deposits and occurrences: A review

L.A. Groat [a,*], G. Giuliani [b], D.D. Marshall [c], D. Turner [a]

[a] Department of Earth and Ocean Sciences, University of British Columbia, Vancouver, British Columbia, Canada V6T 1Z4
[b] IRD and Centre de Recherches Pétrographiques et Géochimiques/CNRS, UPR 2300, 15 rue Notre Dame des Pauvres, BP 20, 54501 Vandœuvre-lès-Nancy Cedex, France
[c] Department of Earth Sciences, Simon Fraser University, Burnaby, British Columbia, Canada V5A 1S6

ARTICLE INFO

Article history:
Received 29 March 2007
Received in revised form 31 July 2007
Accepted 9 September 2007
Available online 22 April 2008

Keywords:
Emerald deposits
Emerald occurrences
Crystal chemistry
Geochemistry
Production
Stable isotopes
Classification
Exploration

ABSTRACT

Emerald, the green gem variety of beryl, is the third most valuable gemstone (after diamond and ruby). Although it is difficult to obtain accurate statistics, Colombia supplies most (an estimated 60%, worth more than $500,000,000 per year) of the world's emeralds. However there is speculation that the emerald mines in Colombia are becoming depleted. Brazil currently accounts for approximately 10% of world emerald production. Emeralds have also been mined in Afghanistan, Australia, Austria, Bulgaria, China, India, Madagascar, Namibia, Nigeria, Pakistan, South Africa, Spain, Tanzania, the United States, and Zimbabwe.

Because it is difficult to obtain accurate analyses of beryllium, most published analyses of beryl are renormalized on the basis of 18 oxygen and 3 Be atoms per formula unit. The color of emerald is due to trace amounts of chromium and/or vanadium replacing aluminum at the *Y* site; in most cases the Cr content is much greater than that of V. To achieve charge balance, the substitution of divalent cations at the *Y* site is coupled with the substitution of a monovalent cation for a vacancy at a channel site.

Beryl is relatively rare because there is very little Be in the upper continental crust. Unusual geologic and geochemical conditions are required for Be and Cr and/or V to meet. In the classic model, Be-bearing pegmatites interact with Cr-bearing ultramafic or mafic rocks. However in the Colombian deposits there is no evidence of magmatic activity and it has been demonstrated that circulation processes within the host black shales were sufficient to form emerald. In addition, researchers are recognizing that regional metamorphism and tectonometamorphic processes such as shear zone formation may play a significant role in certain emerald deposits.

A number of genetic classification schemes have been proposed for emerald deposits. Most are ambiguous when it comes to understanding the mechanisms and conditions that lead to the formation of an emerald deposit. Studies of individual emerald deposits show that in most cases a combination of mechanisms (magmatic, hydrothermal, and metamorphic) were needed to bring Be into contact with the chromophores. This suggests the need for a more flexible classification scheme based on mode of formation. Stable isotopes can be used to estimate the contribution of each mechanism in the formation of a particular deposit. Such estimates could perhaps be more precisely defined using trace element data, which should reflect the mode of formation.

Emerald may be identified in the field by color, hardness, and form. It will tend to show up in stream sediment samples but because its specific gravity is relatively low, it will not concentrate in the heavy mineral fraction. In Colombia, structural geology, the sodium content of stream sediment samples, and the lithium, sodium, and lead contents of soil samples have all been used to find emerald occurrences. Exploration for gem beryl could result in the discovery of new occurrences of non-gem beryl or other Be minerals that could become new sources of Be and Be oxide.

Future efforts should go towards creating a comprehensive data base of emerald compositions (including trace elements), determination of the role of metamorphism in the formation of some emerald deposits, improved classification schemes, and more effective exploration guidelines.

1. Introduction

Emerald is the green gem variety of beryl ($Be_3^{2+}Al_2^{3+}Si_6^{4+}O_{18}^{2-}$). The color of emerald is due to trace amounts of Cr and/or V replacing Al in the crystal structure. The presence of Cr and V in the beryl structure causes a red fluorescence that enhances the luminosity of the blue-green color, but if Fe^{3+} is present in the emerald crystal, this effect is suppressed (Nassau, 1983). There is some debate over the difference between emerald and green beryl (see Conklin, 2002; Schwarz and Schmetzer, 2002). However, a definition that appears to be attaining broad acceptance is that of Schwarz and Schmetzer (2002): "emeralds

* Corresponding author. Tel.: +1 604 822 4525; fax: +1 604 822 6088.
E-mail address: lgroat@eos.ubc.ca (L.A. Groat).

0169-1368/$ – see front matter © 2008 Elsevier B.V. All rights reserved.
doi:10.1016/j.oregeorev.2007.09.003

are yellowish green, green or bluish green, natural or synthetic beryls, which reveal distinct Cr and/or V absorption bands in the red and blue-violet ranges of their absorption spectra."

Emerald is one of the most valuable gemstones. The highest price ever paid for an emerald was $1,149,850 for an exceptional 10.11 ct Colombian stone in 2000 (Zachovay, 2002). The pricing of emeralds is unique in the colored gemstone market because a greater importance is placed on color rather than clarity, brilliance, or other characteristics (Walton, 2004). In this paper we review the crystal chemistry of beryl, the geochemistry of Be, Cr, and V, production, emerald deposits and occurrences, genetic classification, stable isotopes, exploration, and future research.

2. The crystal chemistry of beryl

Beryl is hexagonal and crystallizes in point group 6/*m*2/*m*2/*m* and space group *P*6/*m*2/*c*2/*c*. The crystal structure is shown in Fig. 1. The Al or *Y* site is surrounded by six O atoms in octahedral coordination, and both the Be and Si sites by four O atoms in tetrahedral coordination. The SiO_4 tetrahedra polymerize to form six-membered rings parallel to (001); stacking of the rings results in large channels parallel to c.

Emerald compositions from the literature are listed in Table 1. Most substitutions occur at the *Y* site. Fig. 2 shows Al versus the sum of other *Y*-site cations for 152 emerald compositions from the literature; as expected, they show an inverse relationship. Fig. 3 shows a slight deviation from a 1:1 correlation between Mg+Mn+Fe and the sum of monovalent cations. This graph suggests that, to achieve charge balance, the substitution of divalent cations for Al at the *Y* site is coupled with the substitution of a monovalent cation for a vacancy at a channel site. There are two sites in the channels; these are referred to as the 2*a* (at 0,0,0.25) and 2*b* (at 0,0,0) positions. Artioli et al. (1993) suggested that, in alkali- and water-rich beryls, H_2O molecules and the larger alkali atoms (Cs, Rb, K) occupy the 2*a* sites and Na atoms occupy the smaller 2*b* positions, but in alkali- and water-poor beryl both Na atoms and H_2O molecules occur at the 2*a* site and the 2*b* site is empty. The amount of water in beryl can be difficult to determine but Giuliani et al. (1997a) derived the following equation from existing experimental data for emerald: H_2O (in wt.%)=[0.84958×Na_2O (in wt.%)]+0.8373.

Points that lie to the right of the 1:1 line in Fig. 3 indicate that some of the Fe in emerald is present as Fe^{3+}. Points that lie above the line could suggest the presence of Li^+ which may substitute for Be^{2+} at the Be site. Charge-balance is maintained by adding a monovalent cation to a channel site. Unfortunately, it is difficult to obtain accurate analyses of Be and Li in beryl. Both are too light to measure with the electron microprobe, which is why most published analyses of beryl are renormalized on the basis of 18 O and 3 Be atoms per formula unit. Beryllium can be analyzed with LA-ICP-MS (Laser Ablation-Inductively Coupled Plasma-Mass Spectrometry), SIMS (Secondary Ionisation Mass Spectrometry, or "ion microprobe"), or by using wet-chemical techniques. However, there is so much Be in the structure that the accuracy of such analyses can be suspect. Lithium may be analyzed by the same techniques as Be, but because the concentrations are much lower the accuracy is not as problematic. The amount of Li can also be estimated in Fe-free beryl from the number of monovalent cations at the channel sites.

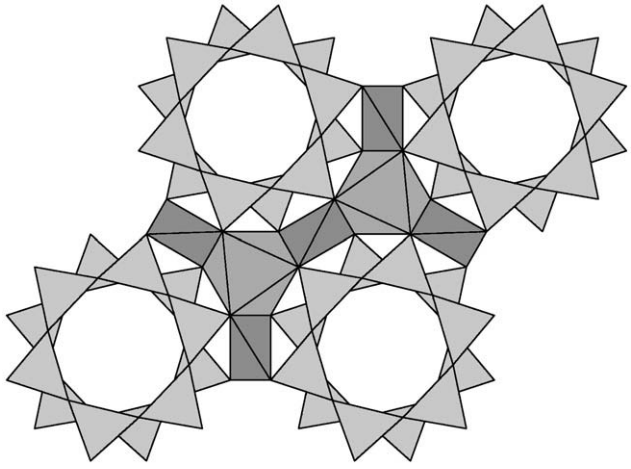

Fig. 1. The crystal structure of beryl projected onto (001), showing BeO_4 tetrahedra (dark grey), AlO_6 octahedra (medium grey), SiO_4 tetrahedra (light grey), and (in this case, empty) channels.

The main substituents for Al at the *Y* site are plotted as oxides in Fig. 4. Magnesium is the main substituent in emeralds from most localities. The elements responsible for most of the variation in color in emerald crystals are plotted as oxides in Fig. 5. In most cases the Cr_2O_3 content is much greater than that of V_2O_3; the main exceptions are for samples from the Lened occurrence in Canada, the Muzo mine in Colombia, the Mohmand district in Pakistan, and Norway.

Beryl has a wide stability field; the lower limit in the presence of water is between 200 and 350 °C, depending on pressure and coexisting minerals (Barton and Young, 2002). However the high-temperature stability and melting relationships remain unclear, partly because beryl may contain significant amounts of H_2O at the channel sites, and water has a significant effect on stability (Zwaan, 2006). The effect of other channel constituents such as Na may be similar. Although thermodynamic data exists for beryl, the lack of experimental data for anything more complex than the BASH ($BeO–Al_2O_3–SiO_2–H_2O$) system can be a barrier to understanding the formation of natural occurrences, such as those where Be-bearing minerals occur in metamorphic rocks (see below) (Zwaan, 2006).

3. The geochemistry of Be, Cr, and V

Beryl is relatively rare because there is very little Be (2.1 ppm; Rudnick and Gao, 2003) in the upper continental crust. Beryllium tends to be concentrated in rocks of the continental crust, such as granites, pegmatites, black shales, and their metamorphic equivalents. Chromium and V are more common (92 and 97 ppm, respectively) in the upper continental crust (Rudnick and Gao, 2003) and are concentrated in dunites, peridotites, and basalts of the oceanic crust and upper mantle, and their metamorphic equivalents. However, high concentrations can also occur in sedimentary rocks, particularly black shales (Schwarz et al., 2002).

Unusual geologic and geochemical conditions are required for Be and Cr and/or V to meet. In the classic model, Be-bearing pegmatites interact with Cr-bearing ultramafic or mafic rocks. However in the Colombian deposits (see below) there is no evidence of magmatic activity and it has been demonstrated that circulation processes within the host black shales were sufficient to form emerald. In addition, researchers are recognizing that regional metamorphism and tectonometamorphic processes such as shear zone formation may play a significant role in certain emerald deposits (see Grundmann and Morteani, 1989, 1993; Nwe and Grundmann, 1990; Cheilletz et al., 2001; Vapnik et al., 2005, 2006; and others). Emeralds, though exceedingly rare, can obviously form in a wider variety of geological environments than previously thought (Walton, 2004).

4. Production

Emeralds, like most colored gemstones, are primarily produced from relatively small, low-cost operations in remote regions of developing countries. As a result it is difficult to obtain accurate statistics regarding production and value. However, even after centuries of production Colombia is still thought to supply an

estimated 60% of the world's emeralds (Schwarz and Giuliani, 2002a). Official production in 2001 was 5.5 million carats (Torres, 2001) worth more than $500 million (Ward, 2001). There is speculation that the emerald mines in Colombia are becoming depleted and there is pressure to discover new reserves (see below). Zambia is considered to be the world's second most important source of emeralds by value; the current total annual emerald production from the Kafubu area is roughly $20 million, in terms of officially declared export values of emerald rough (Zwaan et al., 2005). Brazil currently accounts for approximately 10% of world emerald production (Schwarz and Giuliani, 2002b). Emeralds have also been mined from numerous other countries (see below).

Some of the historical problems facing the emerald sector are due to the fact that deposits are commonly located in countries with unstable political regimes and/or no confirmed security of mineral tenure. Smuggling tends to be rampant and, as with all colored gemstones, there is a lack of industry-wide standards for treatments and disclosure. Despite the problems, emerald continues to be one of the most sought-after colored gemstones in the world.

5. Emerald deposits and occurrences

5.1. Afghanistan

The principal emerald occurrences in Afghanistan lie within a 400 km^2 area centered on the Panjshir Valley 130 km NE of Kabul (Bowersox et al., 1991; Fijal et al., 2004). According to Giuliani et al. (2000a) mining began prior to the 18th Century. Production in 1990 was worth $10 million, and the largest reported cut stone weighed approximately 15 ct (Schwarz and Giuliani, 2002c). Kazmi and Snee (1989) suggested that the emerald occurrences in the Panjshir Valley are related to a continental suture zone. Sabot et al. (2000) described the Tawach deposit (NW of the Panjshir Valley) as being related to the intrusion of tourmaline-bearing leucogranite into serpentinite bodies, which produced weakly developed phlogopite reaction bands containing emerald. The temperature of formation was estimated to be 550 °C. Ar–Ar dating on phlogopite gave a Lower Jurassic age at 193 Ma (Sabot et al., 2002).

Emeralds also occur in the Khendj and adjacent valleys on the SE side of the Panjshir Valley. These occurrences are very different, being hosted by metamorphic schists that have been subjected to intense hydrothermal alteration. The altered zones are irregularly scattered along a fracture network and characterized by the development of albite, muscovite, biotite, tourmaline, and pyrite. Fluid inclusions in the emeralds are highly saline which suggests that the SE Panjshir deposits, like those in Colombia (see below), are linked to hydrothermal fluids that derived their high salinity from leaching of evaporitic sequences (Giuliani et al., 1997a; Sabot et al., 2000; Vapnik and Moroz, 2001; Franz and Morteani, 2002; Giuliani et al., 2005). However, the metamorphic grade of the host rocks is higher than in the Colombian deposits. The hydrothermal fluids resulted from tectonism that preceded uplift during the Himalayan Orogeny (Sabot et al., 2000). Ar–Ar dating on micas gave a Miocene age of 23±1 Ma which correlates with the age of 23.7±1 Ma obtained for the formation of emeralds from Swat in Pakistan (Dilles et al., 1994). Vapnik and Moroz (2001) estimated a crystallization temperature of about 400 °C. Schwarz and Giuliani (2002c) pointed out that although the chromophores likely originated from the host rocks the source of the Be remains unknown.

5.2. Australia

Emeralds were first discovered in Australia in an abandoned tin deposit near Emmaville in northern New South Wales in 1890 (compositions of Australian emeralds are shown in Fig. 6). Out of 25,000 ct originally mined, only 0.01 to 0.02% were of gem-quality. Since then the mine has been re-opened and closed several times (Walton, 2004). The Emmaville and nearby Torrington deposits are related to the intrusion of pegmatites and aplites into mudstones and siltstones (Mumme, 1982; Kazmi and Snee, 1989; Schwarz, 1991). At Emmaville the emeralds are in pegmatite dikes with fluorite, beryl, quartz, topaz, arsenopyrite, and cassiterite. The crystals are embedded in granitic cavities that have weathered to kaolinite. At the Torrington occurrence the emeralds occur in quartz and pegmatite veins and are associated with quartz, feldspar, biotite, and wolframite. The H isotopic composition of the fluids trapped by the emeralds indicates a magmatic origin (Groat et al., 2002).

Australia's most productive emerald district is a 10 km^2 area around the village of Poona in Western Australia (Mumme, 1982; Kazmi and Snee, 1989). Light green emerald occurs with ruby, chrysoberyl ($BeAl_2O_4$), sapphire, topaz, fluorite, margarite, muscovite, and quartz in a phlogopite “blackwall” zone, interpreted as a product of metasomatic reactions (under low-grade metamorphic conditions) between pre-existing quartz–muscovite or quartz–topaz greisens and ultramafic bodies (Grundmann and Morteani, 1995). The chrysoberyl crystals show the alexandrite effect in which they appear green to blue green in daylight and violet-red in incandescent light.

At Menzies in Western Australia, emeralds are found associated with a series of pegmatite dikes which are concordantly emplaced along schistosity planes within ultramafic rocks (Garstone, 1981). The host schist formed through K metasomatism of the ultramafic rock during intrusion of the pegmatite. Beryl is found in the pegmatite but is more abundant in the mica schist. Garstone (1981) recognized three stages of beryl crystallization: (1) colorless and pale green beryls; (2) dark green beryl and emerald containing 0.15 to 0.23 wt.% Cr_2O_3; (3) alkali-rich, Cr-deficient beryl.

A small number of emeralds have also been recovered from the Wodgina tantalum mine in Western Australia (Schwarz, 1991).

5.3. Austria

The emerald deposit at Leckbachscharte in the Habachtal (Hohe Tauern, Salzburg) may have been mined by the Romans or even the Celts. The mine is now dormant. The emerald deposit is situated in the Habach Formation, which consists of a sequence of metapelites and metavolcanics with interlayered serpentinites, near the contact with the Zentral gneiss. The emeralds occur within metasomatic biotite schists called “blackwall” zones developed between these rocks as a result of regional metamorphism involving intense deformation. Emerald porphyroblasts grew syn- to post-tectonically, mainly at the contact between muscovite-plagioclase-chlorite boudins and biotite schists. Geochemical analyses show that the entire “blackwall” zone is enriched in Be, which Grundmann and Morteani (1989) suggest originated with submarine volcanic exhalations. Mass balance calculations suggest that the transformation of the metapelites-metavolcanics and serpentinites replaced Be-rich silicates such as muscovite by biotite and chlorite, which released excess Be to form beryl. The source of the Cr is the metasomatized ultrabasic rocks (Grundmann and Morteani, 1989).

Grundmann and Morteani (1989) argued for a regional metamorphic origin for the emeralds based on the following evidence: (1) augen textures in the country rocks; (2) strongly zoned emeralds with sigmoidal inclusion trails, indicating polystage growth with simultaneous deformation; (3) no evidence of contact mineralization; (4) the REE fractional pattern and Yb/Ca vs. Tb/Ca ratios of coexisting fluorite indicate the existence of an abundant non-pegmatitic fluid phase during formation of the emeralds. In addition, fluid inclusions in the emerald show similar characteristics to those in syn-metamorphic Alpine fissures in the Habach Formation (Grundmann and Morteani, 1989), and reveal at least four phases of deformation (Nwe and Grundmann, 1990), evidence for regional metamorphism and syntectonic growth.

Table 1
Emerald compositions from the literature

	1	2	3	4	5	6	7	8	9	10	11	12	13	14	15	16	17	18	19	20	21	22	23	24	25	26	27
SiO_2	66.0	67.1	65.1	67.22	67.43	67.12	67.50	67.13	64.95	66.01	65.39	65.36	64.23	66.81	66.65	65.40	65.92	66.71	66.17	65.68	64.67	66.64	66.60	64.67	65.49	64.40	63.54
Al_2O_3	18.2	18.2	17.1	18.47	18.15	18.42	17.86	17.83	16.63	17.31	16.48	16.66	16.47	17.56	17.55	17.63	16.91	17.35	17.29	17.21	17.73	16.58	18.23	18.00	18.09	18.03	17.25
Sc_2O_3	n.d.	n.d.	n.d.	-	-	-	-	-	-	-	-	-	-	-	-	-	-	-	-	-	-	-	-	-	-	-	-
V_2O_3	0.08	0.07	0.03	0.08	0.12	0.09	0.08	0.13	bdl	bdl	0.02	bdl	0.02	0.05	0.06	0.02	0.04	0.04	0.05	0.08	0.02	0.05	0.03	0.04	0.02	-	-
Cr_2O_3	0.19	0.23	0.10	0.15	0.09	0.11	0.10	0.04	0.22	0.23	0.15	0.27	0.15	0.07	0.09	0.19	0.38	0.18	0.26	0.55	0.19	0.44	0.11	0.26	0.15	0.23	0.12
BeO	*13.76*	*14.13*	*13.55*	*13.95*	*13.94*	*13.94*	*13.91*	*13.85*	*13.49*	*13.71*	*13.52*	*13.56*	13.07	*13.82*	*13.80*	*13.55*	*13.56*	*13.74*	*13.67*	*13.64*	*13.47*	*13.80*	*13.85*	*13.54*	*13.67*	14.28	13.07
MgO	0.22	0.31	0.75	0.05	0.05	0.03	0.06	0.06	0.82	0.57	0.71	0.72	1.04	0.36	0.36	0.15	0.19	0.20	0.26	0.53	0.18	0.92	0.21	0.35	0.20	0.52	0.84
CaO	-	-	-	bdl	bdl	0.02	bdl	0.01	bdl	0.02	0.02	bdl	0.00	bdl	bdl	0.02	bdl	bdl	bdl	0.02	bdl	bdl	bdl	0.03	bdl	0.16	0.78
MnO	-	-	-	bdl	bdl	bdl	bdl	bdl	bdl	bdl	bdl	bdl	0.00	bdl	bdl	-	-	-	-	-	-	-	-	-	-	0.19	-
FeO	0.27	2.70	0.46	0.13	0.15	0.24	0.16	0.25	0.47	0.30	0.45	0.63	0.94	0.30	0.28	0.10	0.14	0.14	0.18	0.07	0.41	0.43	0.16	0.16	0.46	0.45	0.64
Na_2O	0.21	0.30	0.70	0.06	0.07	0.06	0.06	0.08	0.86	0.74	0.79	0.79	1.44	0.39	0.47	0.21	0.29	0.27	0.36	0.39	0.24	0.89	0.27	0.45	0.31	0.48	1.42
K_2O	-	-	-	bdl	bdl	0.03	bdl	bdl	0.02	bdl	bdl	bdl	0.07	bdl	0.02	0.01	0.01	0.03	bdl	bdl	bdl	0.03	bdl	0.03	0.02	0.14	0.14
Cs_2O	-	-	-	-	-	-	-	-	-	-	-	-	0.14	-	-	-	-	-	-	-	-	-	-	-	-	-	-
H_2O	*1.02*	*1.09*	*1.43*	*0.89*	*0.90*	*0.89*	*0.89*	*0.91*	*1.57*	*1.47*	*1.51*	*1.51*	2.03	*1.17*	*1.24*	*1.02*	*1.08*	*1.07*	*1.14*	*1.17*	*1.04*	*1.59*	*1.07*	*1.22*	*1.10*	1.60	2.97
Total	99.95	104.13	99.22	101.00	100.90	100.95	100.62	100.29	99.03	100.36	99.04	99.50	99.65	100.53	100.52	98.30	98.52	99.73	99.38	99.34	97.95	101.37	100.53	98.75	99.51	100.48	100.77
Si^{4+}	5.991	5.930	5.999	6.016	6.040	6.015	6.060	6.052	6.013	6.011	6.042	6.020	5.988	6.038	6.032	6.027	6.069	6.063	6.046	6.015	5.996	6.029	6.007	5.964	5.984	5.876	5.920
Al^{3+}	1.947	1.896	1.857	1.948	1.916	1.945	1.890	1.895	1.815	1.858	1.795	1.808	1.810	1.870	1.872	1.915	1.835	1.858	1.862	1.858	1.937	1.768	1.938	1.956	1.948	1.939	1.894
Sc^{3+}	n.d.	n.d.	n.d.	-	-	-	-	-	-	-	-	-	-	-	-	-	-	-	-	-	-	-	-	-	-	-	-
V^{3+}	0.006	0.005	0.002	0.006	0.009	0.006	0.006	0.009	bdl	bdl	0.001	bdl	0.001	0.004	0.004	0.001	0.003	0.003	0.004	0.006	0.001	0.004	0.002	0.003	0.001	-	-
Cr^{3+}	0.014	0.016	0.007	0.011	0.006	0.008	0.007	0.003	0.016	0.017	0.011	0.020	0.011	0.005	0.006	0.014	0.028	0.013	0.019	0.040	0.014	0.031	0.008	0.019	0.011	0.017	0.009
Be^{2+}	*3.000*	*3.000*	*3.000*	*3.000*	*3.000*	*3.000*	*3.000*	*3.000*	*3.000*	*3.000*	*3.000*	*3.000*	2.927	*3.000*	*3.000*	*3.000*	*3.000*	*3.000*	*3.000*	*3.000*	*3.000*	*3.000*	*3.000*	*3.000*	*3.000*	3.130	2.925
Mg^{2+}	0.030	0.041	0.103	0.007	0.007	0.004	0.008	0.008	0.113	0.077	0.098	0.099	0.145	0.049	0.049	0.021	0.026	0.027	0.035	0.072	0.025	0.124	0.028	0.048	0.027	0.071	0.117
Ca^{2+}	-	-	-	bdl	bdl	0.002	bdl	0.001	bdl	0.002	0.002	bdl	0.000	bdl	bdl	0.002	bdl	bdl	bdl	0.002	bdl	bdl	bdl	0.003	bdl	0.016	0.078
Mn^{2+}	-	-	-	bdl	bdl	bdl	bdl	bdl	bdl	bdl	bdl	bdl	0.000	bdl	bdl	-	-	-	-	-	-	-	-	-	-	0.015	-
Fe^{2+}	0.020	0.200	0.035	0.010	0.011	0.018	0.012	0.019	0.036	0.023	0.035	0.049	0.073	0.023	0.021	0.008	0.011	0.011	0.014	0.005	0.032	0.033	0.012	0.012	0.035	0.034	0.050
Na^{+}	0.037	0.051	0.125	0.010	0.012	0.010	0.010	0.014	0.154	0.131	0.142	0.141	0.260	0.068	0.082	0.038	0.052	0.048	0.064	0.069	0.043	0.156	0.047	0.080	0.055	0.085	0.256
K^{+}	-	-	-	bdl	bdl	0.003	bdl	bdl	0.002	bdl	bdl	bdl	0.008	bdl	0.002	0.001	0.001	0.003	bdl	bdl	bdl	0.003	bdl	0.004	0.002	0.016	0.017
Cs^{+}	-	-	-	-	-	-	-	-	-	-	-	-	0.006	-	-	-	-	-	-	-	-	-	-	-	-	-	-

Calculated values are italicized. In most cases the compositions were recalculated on the basis of 3 Be and 18 O apfu. Calculated H_2O = (0.84958 × Na_2O) + 0.8373 (Giuliani et al., 1997a).

1-3. Afghanistan, Panjsher (Hammarstrom, 1989).

4-8. Australia, Emmaville (Schwarz, 1991).

9-12. Australia, Menzies (Schwarz, 1991).

13. Australia, Menzies (Garstone, 1981). Includes 0.05 wt.% Li_2O, 2.01 wt.% H_2O^+, 0.02 wt.% H_2O^-.

14-15. Australia, Poona (Schwarz, 1991).

15-25. Australia, Poona (Schwarz, 1991).

26. Australia, Poona (Simpson, 1948).

27. Austria, Salzburg (Leitmeier, 1937).

Table 1 (*continued*)

	28	29	30	31	32	33	34	35	36	37	38	39	40	41	42	43	44	45	46	47	48	49	50	51	52	53	54	55
SiO_2	61.94	61.64	63.63	65.11	65.06	65.28	64.98	63.88	63.98	64.55	63.83	64.09	64.46	65.44	64.66	64.89	64.18	65.35	65.55	65.36	64.75	65.26	65.07	65.25	*65.14*	*65.14*	*65.14*	*65.14*
Al_2O_3	14.39	13.70	15.95	16.25	17.12	17.46	17.52	16.06	15.79	15.65	15.34	16.25	15.55	17.10	17.78	18.10	17.04	18.78	18.38	18.82	18.84	17.60	18.51	17.62	*18.20*	*18.20*	*18.20*	*18.20*
Sc_2O_3	-	-	-	-	0.03	0.01	0.01	0.08	0.06	0.03	0.00	0.04	0.02	0.01	-	-	-	-	-	-	-	-	-	-	-	-	-	-
V_2O_3	0.07	0.06	-	-	0.29	0.20	0.02	0.04	0.05	0.02	0.00	0.02	0.02	0.02	0.12	0.12	0.13	0.10	0.05	0.01	0.01	-	-	-	-	0.04	-	-
Cr_2O_3	0.9	0.72	0.004	0.11	0.00	0.00	0.00	0.45	0.45	1.14	0.41	0.36	0.52	0.01	0.34	0.28	0.22	0.16	0.12	0.07	0.01	0.08	0.13	0.26	-	-	0.03	-
BeO	*13.06*	*12.90*	13.10	*13.53*	*13.59*	*13.64*	*13.56*	*13.32*	*13.34*	*13.43*	*13.27*	*13.38*	*13.41*	*13.60*	12.85	12.97	13.66	13.59	13.37	13.27	13.75	13.20	12.65	*13.89*	*12.82*	*12.82*	*12.82*	*12.82*
MgO	2.81	2.77	1.00	1.29	0.93	0.80	0.61	1.16	1.35	1.12	1.69	1.15	1.54	0.65	1.65	1.24	1.61	0.74	0.94	0.82	0.74	0.77	0.24	0.43	0.83	0.80	0.87	0.83
CaO	0.01	0.00	1.53	0.03	0.00	0.00	0.01	0.02	0.03	0.02	0.07	0.02	0.04	0.02	0.00	0.01	0.02	0.01	0.00	0.01	0.00	0.69	0.63	-	-	-	-	-
MnO	0.00	0.00	-	0.02	-	-	-	-	-	-	-	-	-	-	0.03	0.05	0.03	0.00	0.01	0.00	0.00	0.06	0.02	-	-	-	-	-
FeO	0.64	1.08	0.43	0.47	0.38	0.32	0.33	0.44	0.47	0.50	0.46	0.61	0.54	0.45	0.26	0.39	0.60	0.14	0.28	0.22	0.24	0.08	0.65	0.90	0.08	0.06	0.05	0.07
Na_2O	1.65	1.50	0.90	1.16	0.84	0.76	0.65	1.02	1.09	1.00	1.18	0.99	1.25	0.78	1.50	1.12	1.41	0.70	0.84	0.76	0.76	0.50	0.43	-	0.69	0.67	0.65	0.66
K_2O	0.02	0.02	0.01	0.01	0.01	0.00	0.02	0.02	0.02	0.03	0.00	0.01	0.03	0.01	0.05	0.07	0.09	0.04	0.04	0.04	0.03	0.22	0.16	-	-	0.02	0.02	-
Cs_2O	-	-	0.06	-	0.15	0.08	0.07	0.15	0.11	0.15	0.07	0.16	0.12	0.22	-	-	-	-	-	-	-	-	-	-	-	-	-	-
H_2O	*2.24*	*2.11*	1.16	*1.82*	*1.55*	*1.48*	*1.39*	*1.70*	*1.76*	*1.69*	*1.84*	*1.68*	*1.90*	*1.50*	0.70	0.60	0.86	0.60	0.74	0.59	0.60	1.84	1.81	1.55	*1.42*	*1.41*	*1.39*	*1.40*
Total	97.73	96.50	97.77	99.80	99.95	100.03	99.17	98.34	98.50	99.33	98.16	98.76	99.40	99.81	100.04	100.05	100.12	100.27	100.54	100.12	99.90	100.57	100.30	99.90	99.18	99.16	99.17	99.12
Si^{4+}	5.925	5.968	5.987	6.008	5.975	5.974	5.986	5.989	5.995	6.002	6.006	5.984	5.980	6.010	5.921	5.924	5.876	5.914	5.934	5.929	5.879	5.983	5.991	5.992	*5.942*	*5.943*	*5.941*	*5.944*
Al^{3+}	1.622	1.563	1.769	1.767	1.853	1.884	1.902	1.775	1.744	1.715	1.701	1.788	1.770	1.851	1.919	1.947	1.839	2.003	1.961	2.012	2.016	1.902	2.008	1.907	*1.957*	*1.957*	*1.956*	*1.957*
Sc^{3+}	-	-	-	-	0.002	0.001	0.001	0.007	0.005	0.002	0.000	0.003	0.001	0.001	-	-	-	-	-	-	-	-	-	-	-	-	-	-
V^{3+}	0.005	0.005	-	-	0.021	0.015	0.001	0.003	0.004	0.001	0.000	0.001	0.001	0.001	0.009	0.009	0.010	0.007	0.004	0.001	0.001	-	-	-	-	0.003	-	-
Cr^{3+}	0.068	0.055	0.000	0.008	0.000	0.000	0.000	0.033	0.033	0.084	0.031	0.027	0.036	0.001	0.025	0.020	0.016	0.011	0.009	0.005	0.001	0.006	0.009	0.019	-	-	0.002	-
Be^{2+}	*3.000*	*3.000*	2.961	3.000	*3.000*	*3.000*	*3.000*	*3.000*	*3.000*	*3.000*	*3.000*	*3.000*	*3.000*	*3.000*	2.827	2.844	3.004	2.954	2.908	2.891	2.999	2.907	2.798	*3.000*	*3.000*	*3.000*	*3.000*	*3.000*
Mg^{2+}	0.401	0.400	0.140	0.177	0.128	0.109	0.084	0.162	0.189	0.155	0.237	0.160	0.190	0.089	0.225	0.169	0.220	0.100	0.127	0.111	0.100	0.105	0.033	0.059	0.113	0.109	0.118	0.113
Ca^{2+}	0.001	0.000	0.154	0.003	0.000	0.000	0.001	0.002	0.003	0.002	0.007	0.002	0.004	0.002	0.000	0.001	0.002	0.001	0.000	0.001	0.000	0.068	0.062	-	-	-	-	-
Mn^{2+}	0.000	0.000	-	0.002	-	-	-	-	-	-	-	-	-	-	0.002	0.004	0.002	0.002	0.001	0.000	0.000	0.005	0.002	-	-	-	-	-
Fe^{2+}	0.051	0.087	0.034	0.036	0.029	0.024	0.025	0.034	0.037	0.039	0.036	0.048	0.034	0.035	0.020	0.030	0.046	0.011	0.021	0.017	0.018	0.006	0.050	0.069	0.006	0.005	0.004	0.005
Na^{+}	0.306	0.282	0.164	0.208	0.150	0.135	0.116	0.185	0.198	0.180	0.215	0.179	0.226	0.139	0.266	0.198	0.250	0.123	0.147	0.134	0.134	0.089	0.077	0.000	0.122	0.119	0.115	0.117
K^{+}	0.002	0.002	0.001	0.000	0.001	0.000	0.002	0.002	0.002	0.004	0.000	0.001	0.004	0.001	0.006	0.008	0.011	0.005	0.005	0.005	0.003	0.026	0.019	0.000	-	0.002	0.002	-
Cs^{+}	-	-	0.002	-	0.006	0.003	0.003	0.006	0.004	0.006	0.003	0.006	0.005	0.009	-	-	-	-	-	-	-	-	-	-	-	-	-	-

28. Brazil (Gavrilenko and Pérez, 1999).
29. Brazil, Santa Terezinha (Gavrilenko et al., 2006).
30. Bulgaria, Urdini Lakes, Rila Mountains (Petrusenko et al., 1966). Includes 0.002 wt.% Rb_2O.
31. Bulgaria, Rila (Alexandrov et al., 2001). Average of 10 analyses.
32-33. Canada, Lened (Marshall et al., 2004). Each is the average of five analyses.
34-41. Canada, Tsa da Glisza (Groat et al., 2002).
42-45. Colombia, Achiote (Kozlowski et al., 1988). Analysis 42 includes 0.1 wt.% Li_2O; 43, 0.03 wt.% TiO_2, 0.18 wt.% Li_2O; 44, 0.01 wt.% BaO, 0.26 wt.% Li_2O; 45, 0.05 wt.% TiO_2, 0.01 wt.% Li_2O.
46-48. Colombia, Achiote (Kozlowski et al., 1988). Analysis 46 includes 0.01 wt.% TiO_2, 0.21 wt.% Li_2O; 47, 0.15 wt.% Li_2O; 48, 0.01 wt.% TiO_2, 0.16 wt.% Li_2O.
49. Colombia, Achiote (Zambonini and Caglioto, 1928). Includes 0.16 wt.% BaO, 0.105 wt.% Li_2O.
50. Colombia, Achiote (Beus and Mineev, 1972).
51. Colombia, Muzo (Otero Muñoz and Barriga Villalba, 1948).
52-60. Colombia, Muzo (Ottaway, 1991).

Table 1 (*continued*)

	56	57	58	59	60	61	62	63	64	65	66	67	68	69	70	71	72	73	74	75	76	77	78	79	80	81	82	83
SiO_2	*65.14*	*65.14*	*65.14*	*65.14*	*65.14*	*65.14*	*65.14*	*65.14*	*65.14*	*65.14*	*65.14*	*65.14*	*65.14*	*65.14*	63.71	64.80	64.29	64.63	64.39	65.12	66.15	66.12	66.65	66.03	66.18	66.23	66.49	64.99
Al_2O_3	*18.20*	*18.20*	*18.20*	*18.20*	*18.20*	*18.20*	*18.20*	*18.20*	*18.20*	*18.20*	*18.20*	*18.20*	*18.20*	*18.20*	18.24	14.42	12.87	13.90	13.00	19.50	17.56	18.56	18.81	19.02	18.95	18.69	19.34	18.94
Sc_2O_3	-	-	-	-	-	-	-	-	-	-	-	-	-	-	-	-	-	-	-	-	-	-	-	-	-	-	-	-
V_2O_3	0.09	0.10	-	-	-	0.08	0.08	0.08	0.07	-	-	0.09	0.09	0.09	0.40	-	-	-	-	0.07	0.15	0.12	0.07	0.04	0.06	0.09	0.05	0.06
Cr_2O_3	0.07	0.07	0.04	0.04	0.04	0.05	0.06	0.04	-	-	-	0.07	0.06	0.10	0.27	0.08	0.15	0.12	0.16	0.29	1.08	0.23	0.04	0.05	0.20	0.34	0.07	0.20
BeO	*13.76*	*12.82*	*12.82*	*12.82*	*12.82*	*12.82*	*12.82*	*12.82*	*12.82*	*12.82*	*12.82*	*12.82*	*12.82*	*12.82*	*12.82*	*13.50*	13.00	13.30	*13.27*	*13.24*	*13.78*	*13.75*	*13.80*	*13.91*	*13.83*	*13.87*	*13.85*	*13.95*
MgO	0.22	0.65	0.68	0.75	0.80	0.79	0.41	0.35	0.33	0.79	0.82	0.79	0.63	0.65	0.64	0.78	2.28	2.75	2.23	2.81	0.05	0.03	0.02	0.05	0.07	0.06	0.04	0.05
CaO	-	-	-	-	-	-	-	-	-	-	-	-	-	-	0.00	0.02	0.04	-	-	0.00	-	-	-	-	-	-	-	-
MnO	-	-	-	-	-	-	-	-	-	-	-	-	-	-	0.00	0.02	0.02	-	0.01	0.01	0.01	0.01	0.00	0.01	0.01	0.00	0.00	0.01
FeO	0.06	0.05	0.07	0.08	0.05	0.06	0.05	0.04	0.08	0.06	0.06	0.06	0.06	0.05	0.10	0.38	0.96	0.73	1.40	0.24	0.30	0.24	0.25	0.25	0.29	0.26	0.22	0.36
Na_2O	0.52	0.53	0.62	0.62	0.65	0.36	0.29	0.29	0.64	0.62	0.61	0.52	0.53	0.53	0.46	1.50	1.73	1.48	1.71	0.04	0.02	0.05	0.07	0.03	0.04	0.06	0.04	0.05
K_2O	-	-	0.00	0.03	0.03	0.00	0.00	0.00	0.03	0.03	-	0.03	-	-	0.00	0.02	0.03	0.02	0.08	0.01	0.02	0.01	0.01	0.01	0.02	0.01	0.00	0.03
Cs_2O	-	-	-	-	-	-	-	-	-	-	-	-	-	-	-	-	-	-	-	-	-	-	-	-	-	-	-	-
H_2O	*1.28*	*1.29*	*1.36*	*1.36*	*1.39*	*1.14*	*1.08*	*1.08*	*1.38*	*1.36*	*1.36*	*1.28*	*1.29*	*1.29*	*1.23*	*2.11*	*2.31*	*2.09*	*2.29*	*0.87*	*0.85*	*0.88*	*0.90*	*0.86*	*0.87*	*0.89*	*0.87*	*0.88*
Total	98.83	98.88	99.00	99.09	99.11	98.26	98.07	98.02	99.15	99.05	98.98	98.84	98.84	98.86	98.69	98.63	98.45	98.47	99.09	99.98	99.92	100.04	100.76	100.20	100.55	100.46	101.08	99.27
Si^{4+}	*5.952*	*5.950*	*5.948*	*5.944*	*5.944*	*5.972*	*5.977*	*5.980*	*5.943*	*5.945*	*5.948*	*5.952*	*5.952*	*5.951*	5.893	6.086	6.087	6.083	6.073	5.903	6.009	5.983	5.985	5.961	5.960	5.972	5.950	5.935
Al^{3+}	*1.960*	*1.959*	*1.959*	*1.957*	*1.957*	*1.966*	*1.968*	*1.969*	*1.957*	*1.958*	*1.959*	*1.960*	*1.960*	*1.960*	1.988	1.596	1.436	1.542	1.445	2.083	1.880	1.979	1.991	2.024	2.011	1.986	2.040	2.038
Sc^{3+}	-	-	-	-	-	-	-	-	-	-	-	-	-	-	-	-	-	-	-	-	-	-	-	-	-	-	-	-
V^{3+}	0.007	0.007	-	-	-	0.006	0.006	0.006	0.005	-	-	0.007	0.007	0.007	0.030	-	-	-	-	0.005	0.011	0.009	0.005	0.003	0.004	0.007	0.004	0.004
Cr^{3+}	0.005	0.005	0.003	0.003	0.003	0.004	0.004	0.003	-	-	-	0.005	0.004	0.007	0.020	0.006	0.011	0.009	0.012	0.021	0.078	0.016	0.003	0.004	0.014	0.024	0.005	0.014
Be^{2+}	*3.000*	*3.000*	*3.000*	*3.000*	*3.000*	*3.000*	*3.000*	*3.000*	*3.000*	*3.000*	*3.000*	*3.000*	*3.000*	*3.000*	*3.000*	2.933	3.025	*3.000*	*3.000*	*3.000*	*3.000*	*3.000*	*3.000*	*3.000*	*3.000*	*3.000*	*3.000*	*3.000*
Mg^{2+}	0.089	0.093	0.102	0.109	0.107	0.056	0.048	0.045	0.107	0.112	0.108	0.086	0.089	0.087	0.108	0.319	0.388	0.313	0.395	0.007	0.004	0.003	0.007	0.009	0.008	0.005	0.007	0.010
Ca^{2+}	-	-	-	-	-	-	-	-	-	-	-	-	-	-	0.000	0.002	0.004	-	-	0.000	-	-	-	-	-	-	-	-
Mn^{2+}	-	-	-	-	-	-	-	-	-	-	-	-	-	-	0.000	0.002	0.002	-	0.001	0.001	0.001	0.001	0.000	0.001	0.001	0.000	0.000	0.001
Fe^{2+}	0.005	0.004	0.005	0.006	0.004	0.005	0.004	0.003	0.006	0.005	0.005	0.005	0.005	0.004	0.008	0.030	0.076	0.057	0.110	0.018	0.023	0.018	0.019	0.019	0.022	0.020	0.016	0.027
Na^{+}	0.092	0.094	0.110	0.110	0.115	0.064	0.052	0.052	0.113	0.110	0.108	0.092	0.094	0.094	0.082	0.273	0.318	0.270	0.313	0.007	0.004	0.009	0.012	0.005	0.007	0.010	0.007	0.009
K^{+}	-	-	0.000	0.003	0.003	0.000	0.000	0.000	0.003	0.003	-	0.003	-	-	0.000	0.002	0.004	0.002	0.010	0.001	0.002	0.001	0.001	0.001	0.002	0.001	0.000	0.003
Cs^{+}	-	-	-	-	-	-	-	-	-	-	-	-	-	-	-	-	-	-	-	-	-	-	-	-	-	-	-	-

61-69. Colombia, Muzo (Ottaway, 1991).

70. Colombia, Muzo (Gavrilenko et al., 2006).

71-72. Egypt, Sikait (Abdalla and Mohamed, 1999).

73. Egypt, Um Kabu (Abdalla and Mohamed, 1999).

74. Egypt, Um Kabu (Abdalla and Mohamed, 1999).

75. Kazakhstan, Delbegetey (Gavrilenko and Pérez, 1999). Average of 35 analyses.

76-85. Kazakhstan, Delbegetey (Gavrilenko et al., 2006).

Table 1 (*continued*)

	84	85	86	87	88	89	90	91	92	93	94	95	96	97	98	99	100	101	102	103	104	105	106	107	108	109	110	111
SiO_2	66.71	64.53	63.25	62.61	61.67	61.95	62.02	61.45	62.42	63.45	64.71	64.52	63.99	63.63	63.11	64.22	64.56	64.75	64.34	63.42	66.37	67.60	67.47	68.24	65.79	65.31	65.19	64.90
Al_2O_3	19.32	19.24	14.23	14.59	14.11	14.09	14.17	14.39	16.24	11.63	12.68	12.38	14.04	10.96	11.52	13.19	12.46	12.67	12.61	19.29	16.85	17.34	16.85	16.76	17.10	17.24	17.09	17.95
Sc_2O_3	-	-	-	0.00	0.00	0.02	0.03	0.02	-	0.09	0.13	0.06	0.06	0.12	0.21	0.16	0.05	0.05	0.06	-	-	-	-	-	0.02	0.01	0.01	0.01
V_2O_3	0.03	0.12	0.01	0.00	0.00	0.03	0.00	0.00	0.02	0.14	0.24	0.19	0.11	0.47	0.05	0.13	0.18	0.00	0.23	0.18	1.29	0.88	1.53	1.44	0.03	0.03	0.03	0.02
Cr_2O_3	0.09	0.67	0.19	0.27	0.38	0.33	0.30	0.30	0.16	2.17	3.03	3.46	2.18	2.55	2.78	2.51	1.40	1.33	0.75	0.12	0.10	0.25	0.10	0.32	0.76	0.58	0.72	0.43
BeO	*13.68*	*13.98*	*13.68*	*13.12*	*13.16*	*12.97*	*12.98*	*12.99*	*12.90*	*13.19*	*13.30*	*13.55*	*13.48*	*13.38*	*13.32*	*13.23*	*13.42*	*13.47*	*13.51*	*13.31*	*13.49*	*13.71*	*13.95*	*13.90*	*14.03*	*13.79*	*13.71*	*13.68*
MgO	0.07	0.03	0.03	1.96	2.37	2.34	2.44	2.37	2.30	1.76	3.78	2.66	2.83	1.93	3.81	3.49	2.63	3.22	3.22	3.02	0.05	0.11	0.09	0.07	0.08	1.04	1.04	1.00
CaO	-	-	0.00	0.14	0.09	0.18	0.00	0.08	-	0.00	0.00	0.12	0.02	0.12	0.11	0.07	0.15	0.14	0.09	-	0.01	0.01	bdl	0.01	0.00	0.01	0.01	0.20
MnO	0.01	0.01	-	0.00	0.00	0.02	0.00	0.00	0.00	0.00	0.03	0.02	0.13	0.00	0.08	0.01	0.01	0.00	0.00	0.00	0.02	0.02	0.02	0.01	0.02	0.02	0.03	0.04
FeO	0.15	0.20	1.46	0.96	1.26	0.96	0.88	0.95	0.90	1.49	0.87	0.86	0.76	1.51	1.33	0.65	1.72	1.82	1.76	0.69	0.18	0.13	0.10	0.12	0.58	0.53	0.53	0.32
Na_2O	0.02	0.05	1.56	1.53	1.16	1.17	1.69	1.68	1.28	0.56	0.46	0.48	0.43	0.69	0.62	0.42	0.84	0.93	0.85	0.03	0.10	0.07	0.06	0.07	0.90	0.93	0.91	0.80
K_2O	0.01	0.00	0.11	0.47	0.39	0.28	0.45	0.42	0.02	2.28	1.75	1.69	1.09	2.32	2.30	1.62	1.47	1.46	1.21	0.01	0.02	0.01	0.02	0.01	n.d.	n.d.	n.d.	n.d.
Cs_2O	-	-	-	-	-	-	-	-	-	-	-	-	-	-	-	-	-	-	-	-	-	-	-	-	-	-	-	-
H_2O	*0.85*	*0.88*	*2.16*	*2.14*	*1.82*	*1.83*	*2.27*	*2.26*	*1.92*	*1.31*	*1.23*	*1.25*	*1.20*	*1.42*	*1.36*	*1.19*	*1.55*	*1.63*	*1.56*	*0.86*	*0.92*	*0.90*	*0.89*	*0.90*	*1.60*	*1.63*	*1.61*	*1.52*
Total	101.20	99.41	98.05	98.59	97.01	97.10	97.57	96.82	97.91	101.41	101.95	101.34	99.53	101.37	100.27	100.28	101.53	102.04	99.79	98.14	99.73	101.28	101.12	102.01	101.63	101.04	100.81	100.57
Si^{4+}	5.959	5.892	6.019	5.941	5.936	5.961	5.963	5.947	5.911	5.744	5.858	5.842	5.794	5.761	5.713	5.814	5.869	5.886	5.849	5.873	6.044	6.051	6.060	6.073	5.956	5.946	5.949	5.920
Al^{3+}	2.034	2.070	1.596	1.632	1.601	1.598	1.606	1.641	1.813	1.240	1.352	1.321	1.498	1.170	1.228	1.408	1.335	1.358	1.351	2.105	1.809	1.829	1.784	1.758	1.824	1.850	1.838	1.930
Sc^{3+}	-	-	-	0.000	0.000	0.002	0.003	0.002	-	0.007	0.010	0.005	0.005	0.010	0.017	0.013	0.004	0.004	0.005	-	-	-	0.000	0.000	0.002	0.001	0.001	0.001
V^{3+}	0.002	0.009	0.001	0.000	0.000	0.002	0.000	0.000	0.002	0.009	0.015	0.012	0.007	0.028	0.003	0.009	0.010	0.000	0.013	0.013	0.094	0.063	0.110	0.103	0.002	0.002	0.002	0.001
Cr^{3+}	0.006	0.048	0.014	0.020	0.029	0.025	0.023	0.023	0.012	0.155	0.217	0.247	0.157	0.182	0.198	0.180	0.100	0.096	0.054	0.009	0.007	0.018	0.007	0.023	0.054	0.042	0.052	0.031
Be^{2+}	*3.000*	*3.000*	*3.000*	*3.000*	*3.000*	*3.000*	*3.000*	*3.000*	*3.000*	*3.000*	*3.000*	*3.000*	*3.000*	*3.000*	*3.000*	*3.000*	*3.000*	*3.000*	*3.000*	*3.000*	*3.000*	*3.000*	*3.000*	*3.000*	*3.000*	*3.000*	*3.000*	*3.000*
Mg^{2+}	0.004	0.004	0.278	0.335	0.336	0.350	0.340	0.332	0.248	0.510	0.359	0.381	0.260	0.515	0.471	0.355	0.436	0.436	0.409	0.007	0.015	0.012	0.009	0.011	0.140	0.141	0.136	0.094
Ca^{2+}	-	-	0.000	0.014	0.009	0.019	0.000	0.008	-	0.000	0.000	0.012	0.003	0.012	0.012	0.007	0.015	0.013	0.009	-	0.001	0.001	bdl	0.001	0.000	0.001	0.001	0.020
Mn^{2+}	0.001	0.001	-	0.000	0.000	0.002	0.000	0.000	0.000	0.000	0.003	0.001	0.100	0.000	0.006	0.001	0.000	0.000	0.000	0.000	0.002	0.002	0.002	0.001	0.002	0.002	0.002	0.003
Fe^{2+}	0.011	0.015	0.116	0.076	0.101	0.077	0.071	0.077	0.071	0.113	0.066	0.065	0.057	0.114	0.100	0.050	0.131	0.138	0.133	0.053	0.014	0.010	0.008	0.009	0.044	0.040	0.040	0.024
Na^{+}	0.003	0.009	0.288	0.281	0.216	0.218	0.315	0.315	0.235	0.097	0.081	0.084	0.075	0.154	0.109	0.073	0.148	0.163	0.151	0.005	0.018	0.012	0.010	0.012	0.158	0.164	0.161	0.141
K^{+}	0.001	0.000	0.013	0.057	0.048	0.034	0.055	0.052	0.002	0.264	0.202	0.194	0.126	0.267	0.267	0.188	0.170	0.170	0.140	0.001	0.002	0.001	0.002	0.001	n.d.	n.d.	n.d.	n.d.
Cs^{+}	-	-	-	-	-	-	-	-	-	-	-	-	-	-	-	-	-	-	-	-	-	-	-	-	-	-	-	-

86. Madagascar, Ankadilalana mine (Hanni and Klein, 1982).

87-90. Madagascar, Kianjavato, Mananjary (Vapnik et al., 2006). Analysis 87 includes 0.09 wt.% SO_3, 0.08 wt.% TiO_2, 0.18 wt.% NiO; 88, 0.22 wt.% SO_3, 0.26 wt.% TiO_2, 0.24 wt.% Ce_2O_3, 0.10 wt.% NiO; 89, 0.10 wt.% SO_3, 0.13 wt.% La_2O_3, 0.40 wt.% Ce_2O_3, 0.19 wt.% CoO; 90, 0.03 wt.% SO_3, 0.07 wt.% TiO_2, 0.30 La_2O_3.

91. Madagascar, Kianjavato, Mananjary (Vapnik et al., 2006). Includes 0.07 wt.% NiO.

92. Madagascar (Gavrilenko et al., 2006).

93-102. Madagascar, Ianapera (Vapnik et al., 2005). Analysis 93 includes 0.28 wt.% La_2O_3, 0.34 wt.% Ce_2O_3, 0.09 wt.% CoO, 0.50 wt.% Rb_2O; 94, 0.12 wt.% SO_3, 0.02 wt.% TiO_2, 0.19 wt.% La_2O_3, 0.28 wt.% Ce_2O_3; 96, 0.09 wt.% SO_3, 0.07 wt.% TiO_2, 0.05 wt.% NiO; 97, 0.45 wt.% CoO; 98, 0.08 wt.% CoO; 99, 0.06 CoO; 100, 0.10 wt.% SO_3, 0.03 wt.% TiO_2, 0.15 wt.% CoO, 0.17 wt.% NiO; 101, 0.10 wt.% CoO, 0.43 wt.% NiO.

103. Nigeria, Jos (Gavrilenko et al., 2006).

104-105. Norway, Eidsvoll (Schwarz, 1991). Analysis 104 includes 0.04 wt.% TiO_2, 0.01 wt.% Mo_2O_3; 105, 0.02 wt.% TiO_2, 0.01 wt.% Mo_2O_3.

106-107. Norway, Eidsvoll (Schwarz, 1991). Analysis 106 includes 0.03 wt.% TiO_2, 0.08 wt.% Mo_2O_3; 107, 0.01 wt.% TiO_2, 0.01 wt.% Mo_2O_3.

108-112. Pakistan, Khaltaro (Hammarstrom, 1989). Analysis 110 includes 0.01 wt.% TiO_2; 111, 0.02 wt.% TiO_2; 112, 0.04 wt.% TiO_2.

Table 1 (*continued*)

	112	113	114	115	116	117	118	119	120	121	122	123	124	1251	126	127	128	129	130	131	132
SiO_2	63.18	63.18	63.36	63.16	62.91	63.49	62.8	62.4	62.9	63.3	63.4	64.2	64.69	62.23	62.23	61.20	63.52	62.86	63.50	62.23	63.91
Al_2O_3	16.45	14.08	14.29	13.86	14.01	14.60	14.2	13.9	13.5	13.8	13.9	13.7	15.16	15.46	15.46	17.20	17.68	16.35	18.22	15.41	18.88
Sc_2O_3	0.03	n.d.	n.d.	n.d.	n.d.	n.d.	0.17	0.16	0.19	n.d.	n.d.	n.d.	-	-	-	-	-	-	-	-	-
V_2O_3	0.03	0.01	0.04	0.00	0.04	0.05	0.05	0.06	0.06	0.96	0.53	0.73	-	0.03	0.03	-	0.04	0.00	0.06	-	-
Cr_2O_3	0.75	0.40	0.27	0.93	1.07	0.21	0.23	0.35	0.33	0.02	0.04	0.05	0.25	0.58	0.58	0.25	0.37	0.24	0.53	0.33	0.08
BeO	*13.28*	*13.14*	*13.20*	*13.16*	*13.16*	*13.25*	*13.10*	*13.00*	*13.00*	*13.20*	*13.20*	*13.30*	*13.37*	*13.14*	*13.13*	*14.60*	*13.42*	*13.29*	*13.48*	*11.90*	*13.70*
MgO	1.04	2.63	2.70	2.67	2.68	2.62	2.69	2.72	2.64	1.95	2.33	2.15	1.89	2.55	2.55	1.70	0.87	2.12	0.64	0.76	0.83
CaO	0.00	0.01	0.02	0.01	0.01	0.00	-	-	-	-	-	-	0.80	0.02	-	0.17	0.01	-	-	0.31	0.96
MnO	0.06	0.00	0.00	0.00	0.00	0.00	-	-	-	-	-	-	tr	0.00	0.00	-	0.00	0.00	0.00	0.02	0.08
FeO	0.63	0.24	0.25	0.19	0.21	0.23	0.47	0.49	0.47	1.68	1.36	1.50	0.31	0.49	0.49	1.62	0.99	0.51	0.78	0.11	0.69
Na_2O	0.95	2.00	2.04	2.07	2.06	1.98	2.05	2.09	2.03	1.99	2.11	2.11	1.80	1.05	1.05	0.85	0.26	1.08	0.24	2.63	1.45
K_2O	n.d.	n.d.	n.d.	n.d.	n.d.	n.d.	-	-	-	-	-	-	tr	0.02	0.02	-	0.18	0.13	0.16	2.89	0.01
Cs_2O	-	-	-	-	-	-	-	-	-	-	-	-	-	-	-	-	-	-	-	-	-
H_2O	*1.64*	*2.54*	*2.57*	*2.60*	*2.59*	*2.52*	*2.58*	*2.61*	*2.56*	*2.53*	*2.63*	*2.63*	1.29	*1.73*	*1.73*	*1.85*	*1.06*	*1.75*	*1.04*	*2.59*	*1.45*
Total	98.08	98.25	98.74	98.65	98.74	98.95	98.34	97.78	97.68	99.43	99.50	100.37	99.56	97.30	97.27	99.44	98.40	98.33	98.65	98.18	102.04
Si^{4+}	5.941	6.004	5.993	5.993	5.969	5.985	5.975	5.979	6.022	5.994	5.992	6.016	5.984	5.916	5.917	5.810	5.911	5.907	5.885	5.906	5.788
Al^{3+}	1.823	1.577	1.593	1.550	1.567	1.622	1.592	1.570	1.523	1.540	1.548	1.513	1.653	1.732	1.732	1.925	1.939	1.811	1.990	1.724	2.015
Sc^{3+}	0.002	n.d.	n.d.	n.d.	n.d.	n.d.	0.014	0.013	0.016	n.d.	n.d.	n.d.	-	-	-	-	-	-	-	-	-
V^{3+}	0.002	0.001	0.003	0.000	0.003	0.004	0.004	0.005	0.005	0.073	0.040	0.055	-	0.002	0.002	-	0.003	0.000	0.004	-	-
Cr^{3+}	0.056	0.030	0.020	0.070	0.080	0.016	0.017	0.027	0.025	0.001	0.003	0.004	0.018	0.044	0.044	0.019	0.027	0.018	0.039	0.025	0.006
Be^{2+}	*3.000*	*3.000*	*3.000*	*3.000*	*3.000*	*3.000*	*3.000*	*3.000*	*3.000*	*3.000*	*3.000*	*3.000*	*3.000*	*3.000*	*3.000*	*3.000*	*3.000*	*3.000*	*3.000*	*3.000*	*3.000*
Mg^{2+}	0.146	0.373	0.381	0.378	0.379	0.368	0.382	0.388	0.377	0.275	0.328	0.300	0.261	0.361	0.361	0.241	0.121	0.297	0.088	0.108	0.112
Ca^{2+}	0.000	0.001	0.002	0.001	0.001	0.000	-	-	-	-	-	-	0.079	0.002	-	0.017	0.001	-	-	0.032	0.093
Mn^{2+}	0.005	0.000	0.000	0.000	0.000	0.000	-	-	-	-	-	-	tr	0.000	0.000	-	0.000	0.000	0.000	0.002	0.006
Fe^{2+}	0.050	0.019	0.020	0.015	0.017	0.018	0.037	0.039	0.038	0.133	0.107	0.118	0.024	0.039	0.039	0.129	0.077	0.040	0.060	0.009	0.052
Na^{+}	0.173	0.369	0.374	0.381	0.379	0.362	0.378	0.388	0.377	0.365	0.387	0.383	0.323	0.194	0.194	0.156	0.047	0.197	0.043	0.484	0.255
K^{+}	n.d.	n.d.	n.d.	n.d.	n.d.	n.d.	-	-	-	-	-	-	tr	0.002	0.002	-	0.002	0.016	0.019	0.350	0.001
Cs^{+}	-	-	-	-	-	-	-	-	-	-	-	-	-	-	-	-	-	-	-	-	-

113-117. Pakistan, Charbagh, Swat (Hammarstrom, 1989). Analysis 113 includes 0.02 wt.% TiO_2.
118-120. Pakistan, Makhad mine, Swat (Hammarstrom, 1989).
121-123. Pakistan, Gandao, Mohmand (Hammarstrom, 1989).
124. Russia, Urals (Vlasov and Kutakova, 1960).
125. Russia, Urals (Gavrilenko and Pérez, 1999).
126. Russia, Mariinskoye (Gavrilenko et al., 2006).
127. South Africa, Transvaal (Kovaloff, 1928).
128. Tanzania (Gavrilenko and Pérez, 1999).
129. Tanzania, Manyara (Gavrilenko et al., 2006).
130. Tanzania, Sumbawanga (Gavrilenko et al., 2006).
131. Zambia, Miku (Hickman, 1972).
132. Zambia, Kitwe (Graziani et al., 1983).

Table 1 (*continued*)

	133	134	135	136	137	138	139	140	141	142	143	144	145	146	147	148	149	150	151	152
SiO_2	62.72	62.72	65.39	65.24	64.86	63.52	63.21	62.29	63.40	62.44	62.14	63.17	63.08	62.71	63.35	65.0	63.84	62.41	62.66	62.94
Al_2O_3	15.82	15.82	15.42	15.33	14.81	15.81	14.97	13.58	15.96	13.65	13.62	14.09	14.39	13.63	14.62	14.2	19.00	15.14	15.48	13.50
Sc_2O_3	-	-	na	na	na	bdl	0.01	0.03	0.03	bdl	bdl	bdl	bdl	bdl	bdl	-	-	-	-	0.00
V_2O_3	0.03	0.03	0.01	0.04	0.02	0.04	0.02	0.04	0.06	0.02	0.02	0.02	0.02	0.03	0.03	-	-	0.05	0.04	0.05
Cr_2O_3	0.37	0.37	0.08	0.20	0.63	bdl	0.25	0.46	0.25	0.04	0.29	0.15	0.31	0.33	0.70	0.5	0.6	0.69	0.59	0.90
BeO	*12.97*	*12.97*	*13.61*	*13.57*	*13.52*	*13.20*	*13.10*	*12.89*	*13.21*	*12.93*	*12.88*	*13.12*	*13.08*	*12.99*	*13.19*	*13.60*	*13.28*	*13.14*	*13.18*	*13.11*
MgO	2.06	2.06	2.39	2.22	2.47	1.48	1.84	2.36	1.26	2.77	2.68	2.45	2.11	2.90	1.81	3.0	0.75	2.59	2.44	2.57
CaO	0.04	-	bdl	bdl	bdl	0.02	0.02	0.02	0.03	0.03	0.06	0.06	0.05	0.07	0.04	-	-	0.02	-	0.01
MnO	0.00	0.00	bdl	bdl	0.01	na	na	na	na	na	na	na	na	na	na	-	-	0.02	0.00	0.00
FeO	0.95	0.95	0.37	0.34	0.90	0.58	0.72	1.31	0.36	1.11	1.05	1.10	0.96	0.93	1.01	0.45	0.30	0.31	0.34	0.64
Na_2O	1.15	1.15	1.46	1.71	1.36	0.76	0.74	0.98	1.04	0.99	0.94	1.49	1.15	0.86	1.45	2.0	2.03	1.27	1.00	2.17
K_2O	0.01	0.01	bdl	bdl	bdl	0.02	0.03	0.04	0.02	0.26	0.25	0.05	0.04	0.21	0.03	-	0.05	0.02	0.01	0.04
Cs_2O	-	-	na	na	na	0.23	0.06	0.20	0.04	bdl	0.05	0.08	0.11	0.04	0.15	-	-	-	-	0.06
H_2O	*1.81*	*1.81*	*2.08*	*2.29*	*1.99*	*1.48*	*1.47*	*1.67*	*1.72*	*1.68*	*1.64*	*2.10*	*1.81*	*1.57*	*2.07*	*2.54*	*1.07*	*1.92*	*1.69*	*2.68*
Total	97.93	97.89	100.81	100.94	100.57	97.14	96.44	95.87	97.38	95.92	95.62	97.88	97.11	96.27	98.45	101.44	101.02	97.58	97.43	98.71
Si^{4+}	5.920	5.922	6.001	6.000	5.990	6.010	6.026	6.035	5.996	6.031	6.024	6.013	6.021	6.027	5.997	5.989	5.784	5.930	5.936	5.997
Al^{3+}	1.760	1.760	1.668	1.662	1.612	1.763	1.682	1.551	1.779	1.554	1.556	1.581	1.619	1.544	1.631	1.542	2.029	1.696	1.728	1.515
Sc^{3+}	-	-	na	na	na	bdl	0.001	0.003	0.002	bdl	bdl	bdl	bdl	bdl	bdl	-	-	-	-	0.000
V^{3+}	0.002	0.002	0.001	0.003	0.001	0.003	0.002	0.003	0.004	0.001	0.001	0.002	0.002	0.002	0.003	-	-	0.004	0.003	0.004
Cr^{3+}	0.028	0.028	0.006	0.014	0.046	bdl	0.019	0.035	0.019	0.003	0.023	0.011	0.023	0.025	0.053	0.036	0.043	0.052	0.044	0.068
Be^{2+}	*3.000*	*3.000*	*3.001*	*2.999*	*3.000*	*3.000*	*3.000*	*3.000*	*3.000*	*3.000*	*3.000*	*3.000*	*3.000*	*3.000*	*3.000*	*3.000*	*3.000*	*3.000*	3.000	3.000
Mg^{2+}	0.290	0.290	0.327	0.304	0.340	0.208	0.262	0.340	0.178	0.398	0.387	0.347	0.300	0.415	0.256	0.412	0.101	0.367	0.345	0.366
Ca^{2+}	0.004	-	bdl	bdl	bdl	0.002	0.002	0.002	0.003	0.003	0.006	0.006	0.005	0.007	0.004	-	-	0.002	-	0.001
Mn^{2+}	0.000	0.000	bdl	bdl	0.001	na	na	na	na	na	na	na	na	na	na	-	-	0.002	0.000	0.000
Fe^{2+}	0.075	0.075	0.028	0.026	0.070	0.046	0.057	0.106	0.028	0.090	0.085	0.087	0.076	0.075	0.080	0.035	0.023	0.025	0.027	0.051
Na^{+}	0.210	0.211	0.260	0.305	0.244	0.139	0.137	0.185	0.190	0.186	0.176	0.276	0.212	0.160	0.265	0.357	0.357	0.234	0.184	0.400
K^{+}	0.001	0.001	bdl	bdl	bdl	0.002	0.004	0.005	0.002	0.032	0.031	0.006	0.005	0.026	0.003	-	0.006	0.001	0.001	0.005
Cs^{+}	-	-	na	na	na	0.009	0.002	0.008	0.002	bdl	0.002	0.003	0.005	0.001	0.006	-	-	-	-	0.003

133. Zambia (Gavrilenko and Pérez, 1999).
134. Zambia, Kitwe (Gavrilenko et al., 2006).
135. Zambia, Chantete (Zwaan et al., 2005).
136-140. Zambia, Chantete (Zwaan et al., 2005).
141-147. Zambia, Kagem (Zwaan et al., 2005).
148. Zimbabwe, Sandawana (Gübelin, 1958). Includes 0.15 wt.% Li_2O.
149. Zimbabwe, Chingachura (Martin, 1962). Includes 0.1 wt.% Li_2O.
150. Zimbabwe (Gavrilenko and Pérez, 1999).
151. Zimbabwe, Sandawana (Gavrilenko et al., 2006).
152. Zimbabwe, Sandawana (Zwaan, 2006). Includes 0.02 wt.% TiO_2, 0.02 wt.% Rb_2O. Average of 55 analyses.

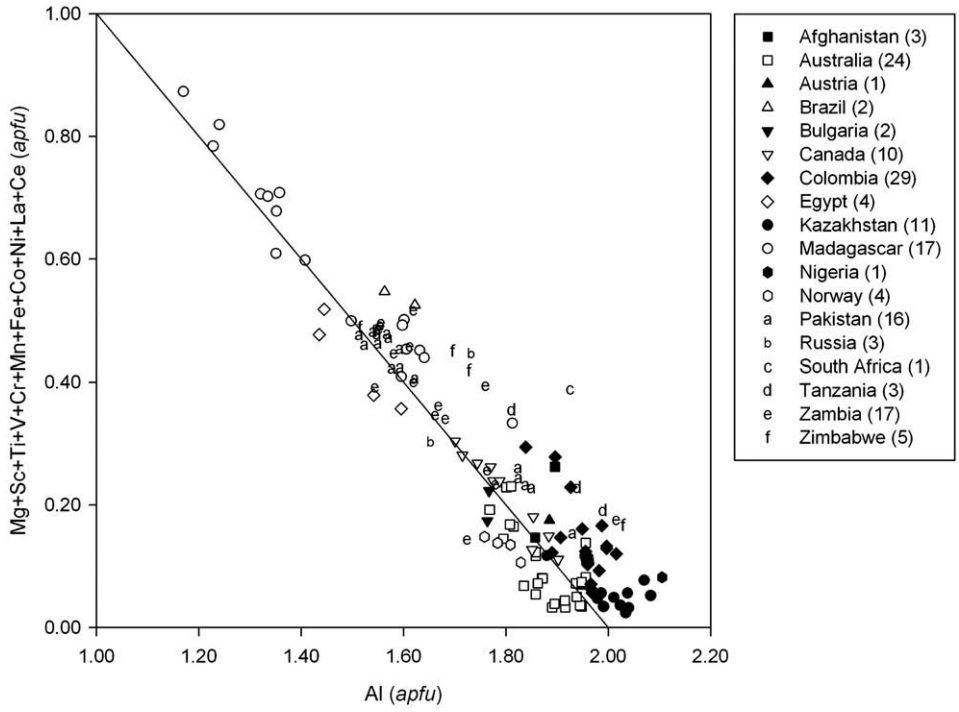

Fig. 2. Al versus the sum of other *Y*-site cations, in atoms per formula unit, for 152 emerald analyses from the literature. The number of analyses per country is given in brackets in the legend. Sources of data: Kovaloff (1928), Zambonini and Caglioto (1928), Leitmeier (1937), Otero Muñoz and Barriga Villalba (1948), Simpson (1948), Gübelin (1958), Vlasov and Kutakova (1960), Martin (1962), Petrusenko et al. (1966), Beus and Mineev (1972), Hickman (1972), Garstone (1981), Hanni and Klein (1982), Graziani et al. (1983), Kozlowski et al. (1988), Hammarstrom (1989), Ottaway (1991), Schwarz (1991), Abdallah and Mohamed (1999), Gavrilenko and Pérez (1999) (Kazakhstan values are averages of 11 analyses), Alexandrov et al. (2001) (average of 10 analyses), Groat et al. (2002), Marshall et al. (2004) (two averages of five analyses each), Vapnik et al. (2005, 2006), Zwaan et al. (2005), Gavrilenko et al. (2006), and Zwaan (2006) (average of 55 analyses).

Zwaan (2006) was critical of this interpretation and warned that in cases where pegmatitic sources of Be are not apparent one must proceed with caution since fluids can travel far from pegmatites, especially along intensely sheared rocks. He also pointed out that pegmatites do occur in the Zentral gneiss, the Habachtal emeralds contain up to 760 ppm Cs (Calligaro et al., 2000), which suggests a pegmatitic source, and sulfide deposits related to submarine volcanic exhalation are not generally enriched in Be (Zwaan, 2006).

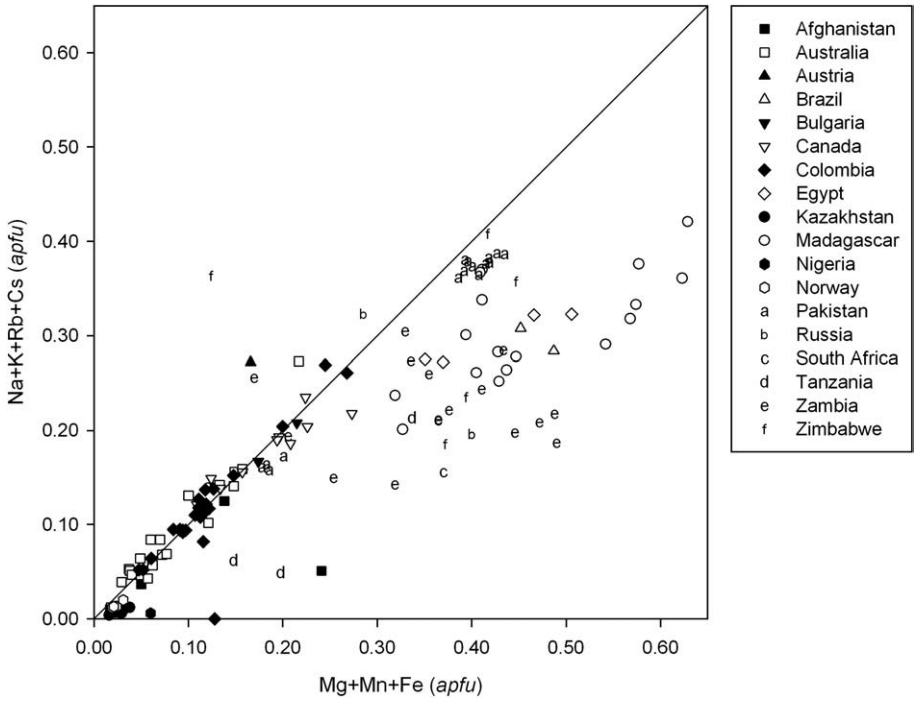

Fig. 3. Mg+Mn+Fe vs. monovalent channel-site cations, in atoms per formula unit, for analyses from the literature. Sources of data are the same as in Fig. 2.

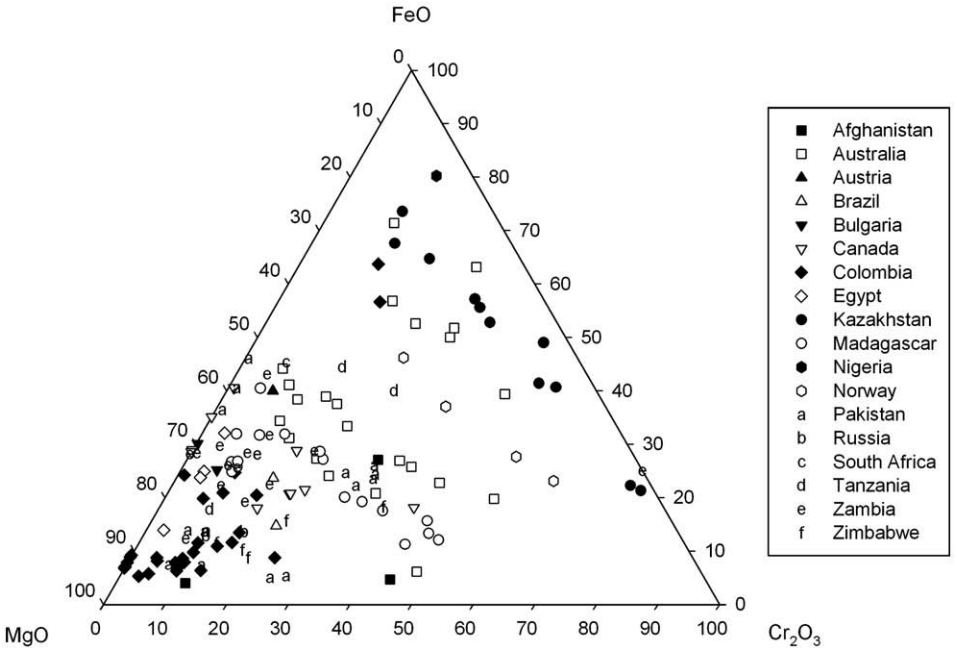

Fig. 4. Plot of emerald compositions in terms of FeO–MgO–Cr_2O_3 (wt.%). Data from the literature (with all Fe as FeO). Sources of data are the same as in Fig. 2. The diagram is after Hammarstrom (1989).

5.4. Brazil

Emeralds were first discovered in Brazil in 1912 at Brumado in Goias State (Just, 1926). They were first exploited in 1963 at Salininha (Cassedanne et al., 1979) and Carnaíba (Couto et al., 1978), both in Bahia State. The main deposits are located in the states of Bahia (Carnaíba and Socotó), Minas Gerais (Mina Belmont, Piteiras, and Capoeirana), and Goiás (Santa Terezinha) (Giuliani et al., 1990). During the, 1980s, Brazil became a significant emerald producer and by the end of the century was exporting $50 million annually in emeralds.

Giuliani et al. (1997a,b) divided Brazilian emerald deposits into two classes. Both are in Proterozoic volcano-sedimentary rocks with intercalations of mafic and ultramafic rocks. Type 1 deposits (all except Santa Terezinha) with emerald grades between 12 and 165 g/t are those in which pegmatites intrude the mafic and ultramafic rocks. The pegmatites have been desilicified and altered to plagioclasites. The mafic and ultramafic rocks were (K, Na) metasomatized to emerald-bearing mica schists (phlogopitites) by hydrothermal fluids channeled by the pegmatites. The Be is almost certainly magmatic in origin. Emerald-bearing quartz veins are also found in several of the deposits.

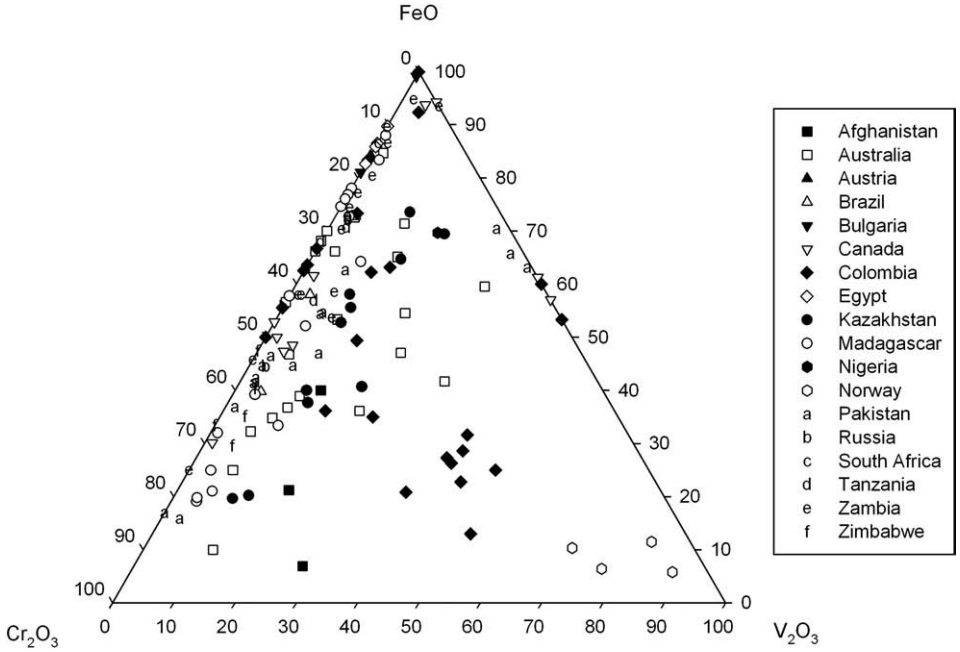

Fig. 5. Plot of emerald compositions in terms of FeO–Cr_2O_3–V_2O_3 (wt.%). Data from the literature (with all Fe as FeO). Sources of data are the same as in Fig. 2. The diagram is after Hammarstrom (1989).

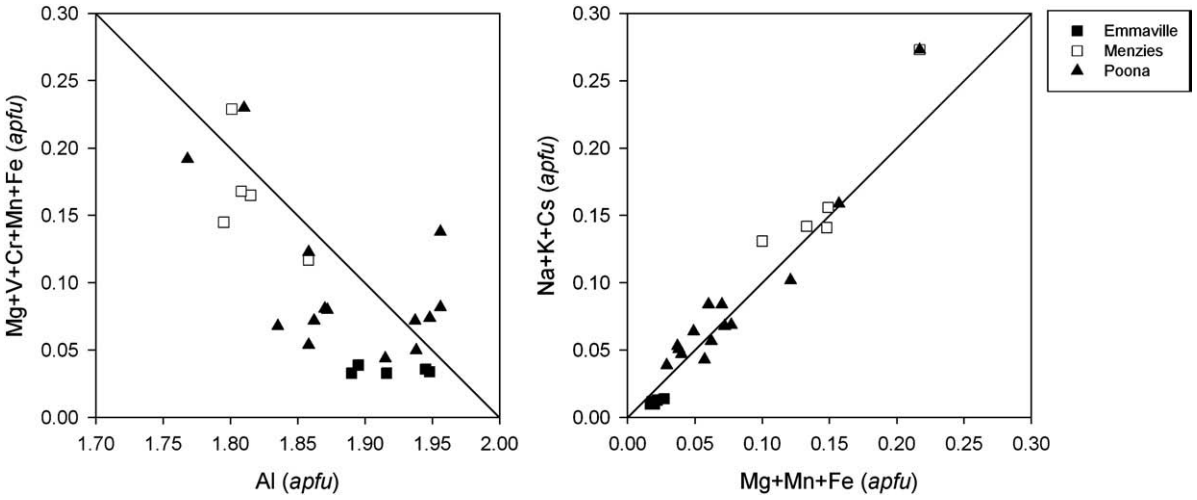

Fig. 6. Compositions of emeralds from Australia. The data are from Simpson (1948), Garstone (1981), and Schwarz (1991).

The Type 2 Santa Terezinha deposit, with emerald grades varying between 50 and 800 g/t, is associated with ductile shear zones cutting mafic and ultramafic rock formations. The emeralds occur in phlogopitites and phlogopitized talc-carbonate schists. The talc schists provided sites for thrusting that gave rise to the formation of sheath folds. Emeralds are most commonly found in the cores of the sheath folds and along the foliations. Isotopic data ($\delta^{18}O$ and δD for emerald and coeval phlogopite) are consistent with both magmatic and metamorphic fluids. However, the absence of granites and related pegmatites, and the low Be concentration in the volcano-sedimentary sequence (<2 ppm), exclude a magmatic origin for Be. A metamorphic origin is therefore proposed for the Santa Terezinha parental fluids.

5.5. Bulgaria

The Rila emerald occurrence in SW Bulgaria is associated with a desilicified pegmatite vein that follows the contact between biotite gneiss and talc schist. Alexandrov et al. (2001) describe the following zoning pattern, which they ascribe to infiltration metasomatism: pegmatite, plagioclase-rich pegmatite, phlogopite schist, amphibole-phlogopite schist, tremolitite, chlorite schist, and talc schist. Emerald is concentrated in the plagioclase-rich parts of the pegmatite and at the contact with the phlogopite zone. Oxygen and H isotopic analyses and fluid inclusion studies of the emerald suggest that a homogeneous fluid of metamorphic origin was responsible for the hydrothermal alteration, which took place at temperatures of 300 to 400 °C (Alexandrov et al., 2001).

5.6. Canada

The Ghost Lake emerald occurrence near Dryden in NW Ontario is associated with a pegmatite which intrudes a chlorite schist. Most of the emerald occurs in a "zone of mixing" between the southern and central limbs of the pegmatites. The rock in the "zone of mixing" consists of relict K-feldspar crystals in a matrix of plagioclase, quartz, phlogopite, apatite, and tourmaline crystals (Garland, 2004). Whole-rock compositions show high concentrations of Be (89 ppm) in the pegmatite and elevated Cr in the chlorite schist (2610 ppm). The emeralds and associated phlogopite most likely formed through metasomatism of the chlorite schist, which was driven by granitic magmatism. Features such as ductile deformation of both the pegmatite and wall zone suggest some degree of shearing, but intrusion of the pegmatite appears to be syndeformational (Brand, 2006).

At the Lened emerald occurrence in the Northwest Territories, a dolomitic limestone has been thrust over a black shale unit (Glover and Burson, 1987). Proximal to the fault the limestone is altered to a pyroxene–garnet±amphibole skarn. The emeralds occur in quartz-carbonate veins which extend from the thrust fault across the skarn and pinch out in the overlying limestone. The black shale footwall unit is devoid of emerald mineralization. The chromophore is V which originates from the black shale, which contains over 3000 ppm V (compositions of Canadian emeralds are shown in Fig. 7). The source of the Be is harder to determine but is most likely a nearby quartz–monzonite stock. Marshall et al. (2004) suggested that hot fluids from the cooling stock traveled along the thrust to produce the contact metamorphic rocks. Prolonged pluton emplacement and cooling resulted in deformation with the calc-silicate rocks behaving in a brittle fashion. This resulted in a set of sub-parallel fractures which became conduits for hydrothermal fluids expelled from the cooling pluton. Quartz and beryl were precipitated in these fractures, resulting in the series of sub-parallel veins.

Emerald was discovered at Tsa da Glisza (formerly Regal Ridge) in the Yukon Territory in 1998. The mineralization is associated with quartz-tourmaline veins and aplite dikes which intrude a chlorite–plagioclase schist. Emerald occurs most commonly along the margins of quartz veins, but is also found within the quartz veins themselves, and in alteration zones that surround the veins. The emerald occurrence is underlain by a granite pluton. Although the Be content of the granite (9.8 to 13.2 ppm) is not anomalously high, the close proximity and the consistent correlation of Be with Sn, W, and Bi in the geochemical data (whole rock and soils) indicate that it is the source of the Be. The Cr in the emerald is most likely from the schist which contains on average 960 ppm Cr (Groat et al., 2002).

Mineralization occurred synchronous with regional deformation and metamorphism related to intrusion of the granite pluton (Neufeld et al., 2004). In particular, mineralization was syn- to late-tectonic, coinciding with the waning stages of granite emplacement, and took place at temperatures of 365 to 498 °C (Marshall et al., 2003). At least two of the aplite dikes contain beryl or emerald, which supports the hypothesis that there is a genetic link between the granite intrusion, aplite and pegmatite bodies, and beryl-bearing quartz veins (Neufeld et al., 2003, 2004; Neufeld, 2004). Chromium entered the fluid system through interaction of the Be-bearing fluids with either hydrothermal fluid which had percolated through the host and extracted Cr, or via element exchange during metasomatic alteration of the vein selvages by the mineralizing fluids.

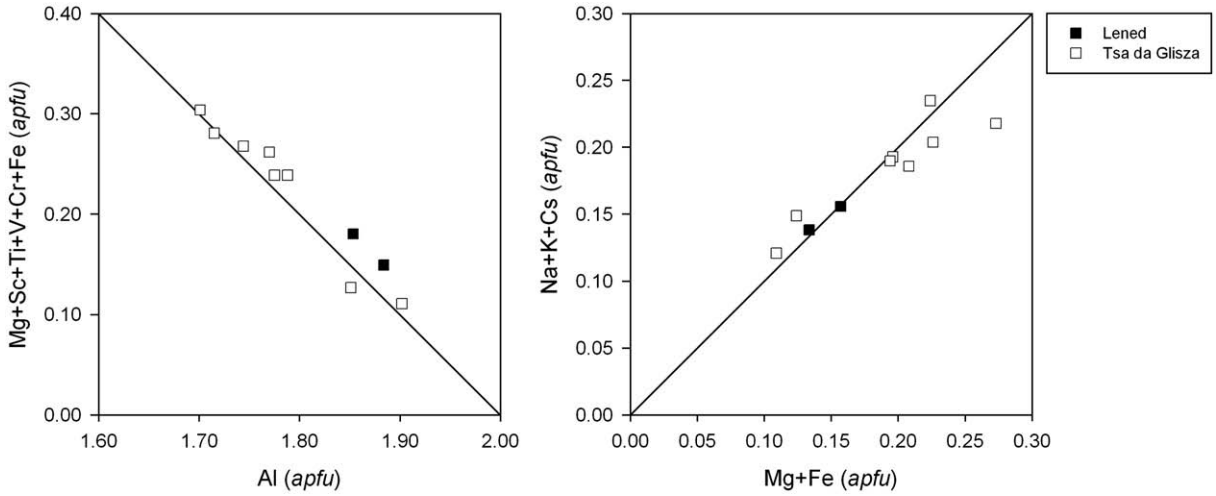

Fig. 7. Compositions of emeralds from Canada. The data are from Groat et al. (2002) and Marshall et al. (2004).

5.7. China

The Dyakou emerald occurrence is in Yunnan Province in southern China. The occurrence is hosted by the Nanwanhe Metamorphic Complex (NMC). The NMC consists of a nucleus and a cover sequence (Feng et al., 1998; Zhang et al., 1998). The nucleus is composed of Neo-Proterozoic metamorphic rocks intruded by Late Silurian orthogneiss and granitic to pegmatitic intrusions. The cover sequence is a series of upper-greenschist to amphibolite-grade meta-sedimentary rocks of Palaeozoic age. Both the nucleus and cover sequences have been intruded by Late Cretaceous evolved granitic rocks.

The V-dominant emeralds occur in quartz and pegmatite veins cutting Proterozoic metamorphic rocks of the Nanyangtian and overlying Saxi units. In general the emeralds in the quartz veins are of better quality, but gem material has also been found in the pegmatite veins. The quartz and pegmatite veins have different orientations, trending NW and NNE, respectively (Zhang et al., 1999). The NW-trending structures formed in the Late Silurian, whereas the NNE-trending structures formed during the Late Cretaceous. This indicates that there may be two separate emerald-forming events, but most likely the emeralds were deposited from CO_2-bearing saline brines (as suggested by NaCl contents of 13 to 18% in fluid inclusions) during the Late Cretaceous, utilizing a pre-existing set of structures, with the Late Cretaceous granitic intrusions and associated pegmatites supplying both heat and Be. In addition, derived pressure-temperature constraints of 325 to 372 °C and 66.7 to 77.9 MPa (Zhang et al., 1999) are consistent with these deposits being of igneous origin. Both vein sets display similar mineralogies with abundant tourmaline and variable amounts of scheelite and fluorite accompanying quartz (±feldspar) in the veins. A slightly reduced sulfide assemblage of arsenopyrite ± pyrrhotite ± pyrite is commonly found within the veins and alteration haloes.

Cr-dominant emeralds have also recently been reported from the Taxkorgan region in western Xinjiang Province, near the village of Dabdar, approximately 120 km from the border with northern Pakistan (Blauwet et al., 2005).

5.8. Colombia

For much of recorded history Colombia has produced the largest and highest quality emerald crystals in the world. The over 200 emerald deposits and occurrences in Colombia are located in two narrow bands on both sides of the Cordillera Oriental, which is the easternmost of three mountain ranges extending from the northern end of the Andes (compositions of Colombian emeralds are shown in Fig. 8). The Guavió–Guatéque mining district, which includes the

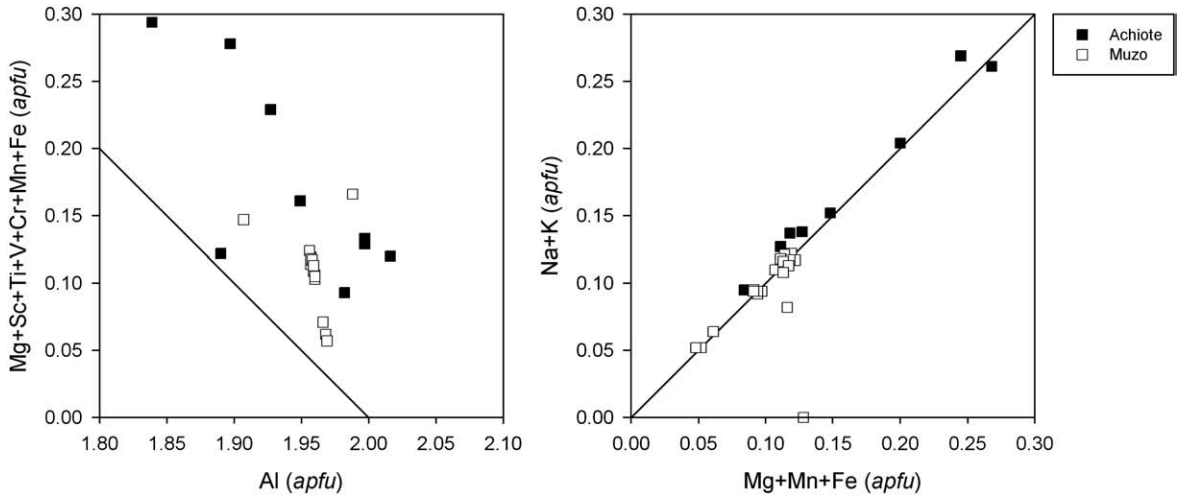

Fig. 8. Compositions of emeralds from Colombia. The data are from Zambonini and Caglioto (1928), Otero Muñoz and Barriga Villalba (1948), Beus and Mineev (1972), Kozlowski et al. (1988), Ottaway (1991) and Gavrilenko et al. (2006).

Chivor, Gachalá, and Macanal deposits is on the eastern flank of the Cordillera Oriental and formed 65 million years ago (Cheilletz et al., 1997). The Vasquez–Yacopí emerald district, comprising the Coscuez, Maripi, Muzo, La Pava, Peñas Blancas, and Yacopí deposits is on the western flank of the Cordillera Oriental. Cheilletz et al. (1994) published estimates of the ages of the Coscuez and Muzo deposits of 35–38 and 32 million years old, respectively (based on $^{40}Ar/^{39}Ar$ data), but Schultz-Güttler and Romero-Ordonez (2000) suggested that, based on Rb/Sr geochemistry, the mineralization at the two mines is coeval. The original Colombian emerald deposits are almost exhausted, but new finds in the Maripi area, beginning with La Pita in 1998, should ensure that Colombia remains the most important source of emeralds for many years to come.

In the Colombian deposits the emeralds occur in extensional carbonate–silicate–pyrite veins, pockets, and breccias in an Early Cretaceous black shale-limestone succession. On the eastern side of the Cordillera Oriental the emerald deposits formed at the time of the Cretaceous–Tertiary boundary during a thin-skinned extensional tectonic event controlled by evaporite dissolution driven by gravity (Branquet et al., 1999a). On the western side of the Cordillera Oriental the emerald deposits are linked by tear faults and associated thrusts developed during a compressive tectonic phase that occurred at the time of the Eocene–Oligocene boundary, prior to the major uplift of the Cordillera during the middle Miocene (Branquet et al., 1999a,b). The mineralization is structurally related to tectonic blocks, 200 to 300 m wide, and emerald mineralization is contained in black shales altered by Na and Ca metasomatism.

The deposits are unusual because there is no evidence for magmatic activity. Instead, the emeralds formed as a result of hydrothermal growth associated with tectonic activity (Ottaway et al., 1994; Giuliani et al., 1995; Cheilletz and Giuliani, 1996; Branquet et al., 1999a,b). A number of studies beginning with Escobar and Mariano (1981) have pointed to an evaporitic origin for the parent hydrothermal fluids. The fluids are thought to have formed at depth from meteoric and formational water interacting with salt beds and evaporitic sequences interbedded with the black shales in the back-arc basins, where they were buried to depths of at least 7 km and reached temperatures of at least 250 °C (Giuliani et al., 2000b). The highly alkaline (up to 40 wt.% NaCl) briny fluids migrated upwards through the sedimentary sequence along décollement thrust planes and then interacted with the black shales. During Na and Ca metasomatism, major elements (Si, Al, K, Ti, Mg, and P) in addition to trace elements (Be, Cr, V, C, B, and U) and REEs were leached from the enclosing black shale; this first stage was accompanied by development of a vein system filled by fibrous calcite, bitumen, and pyrite. The second stage was characterized by extensional vein sets and hydraulic breccia development filled by muscovite, albite, rhombohedral calcite and dolomite, pyrite, bitumen, and by the precipitation in drusy cavities of fluorite, apatite, parisite [$Ca(Ce,La)_2(CO_3)_3F_2$], dolomite, emerald, and quartz. The geochemical model is essentially the same for both emerald districts although they differ in age and tectonic setting (Branquet et al., 1999a).

According to Ottaway et al. (1994), the hydrothermal brines transported evaporitic sulfate to structurally favorable sites, where it was thermochemically reduced by bitumen-derived H_2S to produce native sulfur and pyrite. The sulfur generated by this process reacted with organic matter in the shales to release trapped Cr, V, and Be, which in turn enabled emerald formation (Ottaway et al., 1994). Chielletz and Giuliani (1996) and Giuliani et al. (2000b) emphasized the important role of organic matter in the formation of Colombian emerald deposits, but argued against the production of sulfur by thermochemical sulfate reduction. They proposed a redox reaction involving large organic molecules, a carbonic hydrate, and SO_4^{2-}, that would generate large quantities of HCO_3^- and H_2S, which then reacted with Ca^{2+} and Fe^{2+} (extracted from the black shale by the hydrothermal fluid) to produce calcite and pyrite, which are closely associated with the emeralds in the veins and breccias.

Ottaway (1991) reported a temperature of 325 °C for emerald precipitation at the Muzo deposit. Cheilletz et al. (1994) studied emeralds from the Coscuez mine and observed that they formed at temperatures of 290 to 360 °C and pressures of 1.06 to 1.12 kbars.

Previous studies (Beus, 1979; Ottaway, 1991) have shown that the black shales in the area of the emerald deposits contain approximately 3 ppm Be. Kozlowski et al. (1988) suggested that Be was transported only a short distance to be re-precipitated (in part) in the form of emerald. A local origin is supported by the distinct stratigraphic control of the emerald-bearing veins. The Be may move as hydroxide complexes in acid solution, as proposed by Renders and Anderson (1986), or as carbonate–hydroxy–halide–beryllates in near-neutral to alkaline solutions, as suggested by Govorov and Stunzhas (1963). Giuliani et al. (1999) suggested that the distribution of Be in the different phases of the hydrothermally altered black shale hosting the emerald deposits indicates that Be mobility is associated with the breakdown of Fe–Mn oxyhydroxide phases. The amount of Be that can be mobilized (0.7 ppm) may represent up to 18 wt.% of the total Be contained in the black shale. A mass balance calculation applied to a well-characterized alteration zone of the Chivor mine was used to estimate reserves of 720,000 emeralds, each with a volume of 5 cm^3, or 48.6 million carats in total.

The current model bears resemblance to that of sediment-hosted stratabound and strataform base metal deposits. Giuliani et al. (1995) noted that the brine fluids responsible for emerald formation are remarkably similar to oil-field brines and brines involved in the formation of Mississippi Valley-type Pb–Zn deposits. Ottaway (1991) has proposed that the MVT Pine Point deposit in the Northwest Territories of Canada is a lower-temperature analog of the Muzo emerald deposits.

Nassau (1983) suggested that in general emeralds from Colombia have a more intense color than Fe-bearing emeralds from pegmatitic-ultramafic environments because Fe^{3+} quenches the red fluorescence. Ottaway (1991) suggested that the removal of Fe from the system as pyrite is an important factor in the development of the spectacular color of Colombian emeralds.

Trapiche emeralds are found only in Colombia in the Vasquez–Yacopi emerald district. The name is in allusion to the shape which is reminiscent of the crushing wheels found in sugar cane mills in Colombia (Fig. 9a). Trapiche emeralds occur in black shales or albitized black shales near emerald-bearing veins (Hochleitner, 2002). They consist of a hexagonal prismatic core overgrown with an outer “shell” of emerald with six planar “arms” radiating from the edges of the core. The arms contain inclusions of albite and carbonate but can also contain lesser amounts of bitumen, pyrite, monazite, K-feldspar, epidote, zircon, and apatite (Fig. 9b) (Ohnenstetter et al., 1998). Sunagawa (2005) attributed the trapiche phenomena in both beryl and corundum to skeletal (or dendritic) growth, in which the edges and corners of the crystal grow much faster than the faces.

5.9. Egypt

The earliest known emerald mine is located at Wadi Sikait in Egypt's Eastern Desert (Jennings et al., 1993; Harrell, 2004). Mining probably began toward the end of the 1st century BC with most of the activity occurring in the late 1st Century AD to the 6th Century AD. Mining also occurred at several other sites within a 15 km radius of Wadi Sikait (including Gebel Zabara, Wadi Nugrus, Wadi Abu Rusheid, Wadi Umm Kabu, Wadi Umm Debaa, and Wadi Gimal) but only from the mid-6th Century AD onwards (Harrell, 2004). The emerald deposits occur in a NW-trending band ~45 km long in the Nugrus Shear Zone. The Cr-dominant emeralds are commonly restricted to schists with subordinate slices of amphibolites and serpentinites which overly a biotite orthogneiss. This sequence is intruded

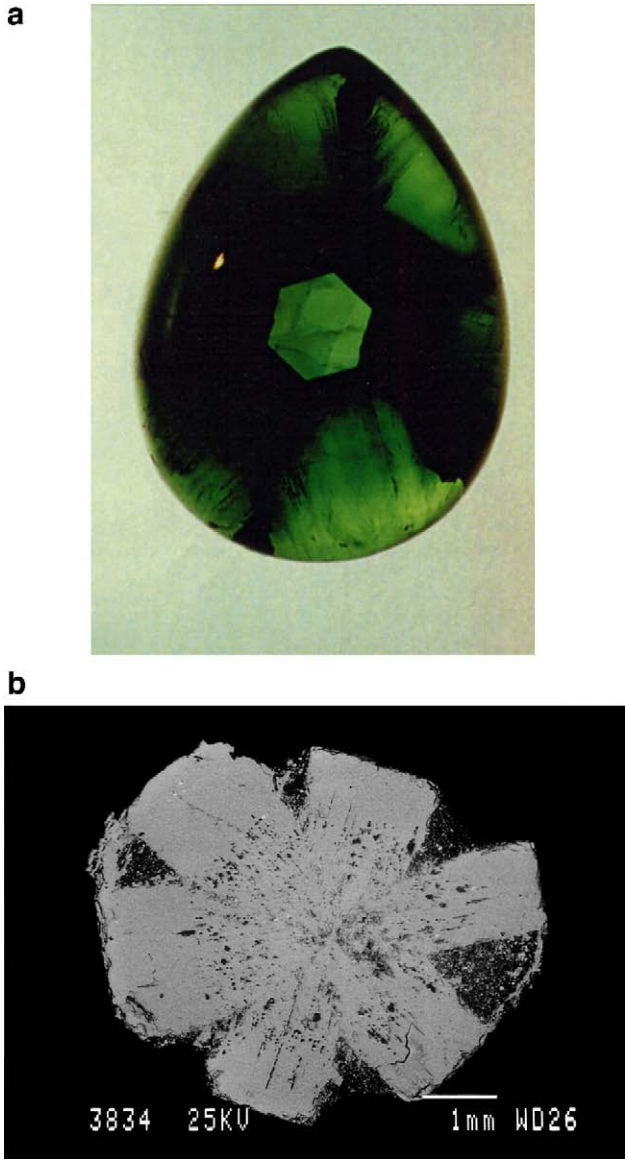

Fig. 9. (a) A 48 ct trapiche emerald crystal from Colombia. (b) a backscattered electron image of a trapiche crystal showing inclusions.

by leucogranite bodies and associated pegmatites (Abdalla and Mohamed, 1999).

At Wadi Sikait emerald occurs in the contact zone between quartz and pegmatite veins in a phlogopite schist (Basta and Zaki, 1961; Abdalla and Mohamed, 1999; Harrell, 2004). The veins, generally only a few cm thick but up to one m in places, are deformed and commonly appear as discontinuous bands and pods. Colorless to white to light green beryl is found in the quartz and pegmatite veins but true emerald is restricted to the schist within tens of cm of the contact.

Fluid inclusions in emeralds from the Egyptian deposits are saline (8 to 22 wt.% NaCl equiv.) and suggest that crystallization took place in the temperature range 260 to 382 °C (Abdalla and Mohamed, 1999). K–Ar dating of phlogopite returned an age of 520 to 580 Ma (Surour et al., 2002). Grundmann and Morteani (1993) suggested that the occurrences resulted from regional metamorphism but this has been challenged by subsequent studies, in particular that of Harrell (2004).

5.10. India

Emerald was first discovered in India in Rajasthan state in 1943. Additional discoveries in the 1940's and 50's defined a belt, 200 km in length, oriented SW to NE between the cities of Ajmer and Udaipur. Emerald-bearing veins occur at the contact between pegmatites and talc schist (metasomatized phyllite; Grundmann and Giuliani, 2002). The best Indian emeralds come from the Rajghar deposit. In 1995 emeralds were also discovered embedded in the wall of a well in the village of Sankari Taluka, in the southern Indian state of Tamil Nadu (Panjikar et al., 1997). These emeralds, which are all Cr-dominant, occur in a lenticular belt of mica schist which has been traced for approximately 5 km. According to Panjikar et al. (1997), similarities in physical properties, compositions, and inclusions between the Sankari emeralds and those from deposits in Madagascar suggest that the former may have been emplaced into Gondwanaland before India rifted from it some 200 million years ago.

5.11. Kazakhstan

In Kazakhstan emeralds are found associated with granite intrusions at Kuu Yuzhnoe and Delbegetey, in the central and NE parts of the country, respectively. The Kuu Yuzhnoe occurrence has no commercial importance but the Delbegetey deposit has been mined since the early 1990's (Gavrilenko et al., 2006). The emerald mineralization at Delbegetey is confined to the southern contact of a granite pluton with hornfelsed Carboniferous sandstones (Vinogradova, 1996). The mineralization is associated with a 2 to 15 m-wide fracture zone oriented E-W with an almost vertical dip. The wallrocks along this zone underwent metasomatism which resulted in the formation of veins composed primarily of quartz, muscovite, tourmaline, fluorite, and beryl (Gavrilenko et al., 2006). Emerald is most commonly found in segregations of mica greisen (up to 0.5 m across) and in quartz–muscovite veins (5 to 20 cm thick). The largest emerald crystals discovered to date are 15 mm in length. Fluid inclusion studies suggest that the emeralds formed at 395 to 420 °C and 570 to 1240 bar (Gavrilenko et al., 2006).

The association of the Delgebetey deposit with sedimentary rocks is unusual for an emerald occurrence associated with granitic magmatism. The source of the Cr is unknown but may be a melange zone containing serpentinites that underlies the sedimentary sequence (E.A. Vinogradova, pers. comm. in Gavrilenko et al., 2006).

5.12. Madagascar

In Madagascar there are two major areas of emerald mineralization: the ~30 km^2 Mananjary region on the east coast and Ianapera in Tulear Province. The compositions of emeralds from the two areas are shown in Fig. 10. The Mananjary deposits are hosted by phlogopite-rich rocks formed through metasomatism of Cr-rich meta-ultrabasites (hornblendites). Beryl generally occurs as euhedral crystals containing up to 2500 ppm Cr (Moine et al., 2004). Moine et al. (2004) studied fluid inclusions in the metasomatic minerals and reported that the alteration took place at 500 °C and 2 kbar. Whole-rock analyses showed that the metasomatism was due to infiltration of F-rich fluids; a thermodynamic model suggested that co-precipitation of F-rich phlogopite was the cause of beryl deposition (Moine et al., 2004). Vapnik et al. (2006) studied fluid inclusions in emeralds from the Kianjavato deposit in the Mananjary region and reported that they formed at 250 to 450 °C and 1.5 kbar. In addition they suggested that shearing was an important mechanism for introducing a CO_2-rich fluid for emerald genesis at the Kianjavato deposit.

The Ianapera deposit is hosted by a Precambrian volcano-sedimentary sequence. The mineralization is located on the flank of an isoclinal fold related to a major N-S shear zone, and occurs in reaction zones developed within lenses of serpentinites and amphibolites. The metasomatic bands are composed of talc masses in tremolite–chlorite lenses. Phlogopite–(rare tourmaline)–quartz–emerald veins are scattered randomly throughout the lenses. Emerald crystals from this locality are small and highly fractured, with colorless

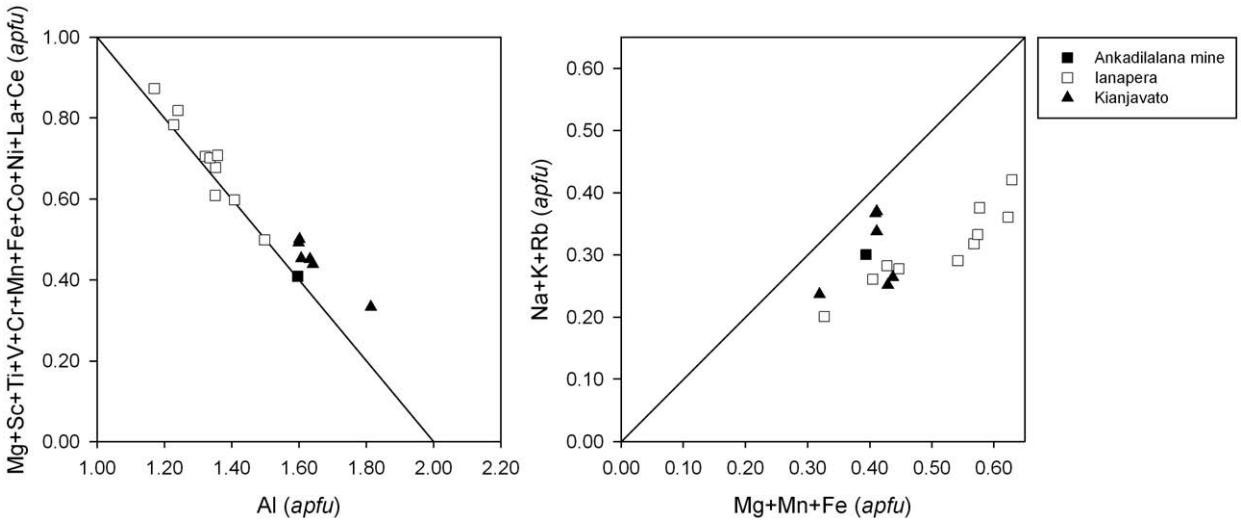

Fig. 10. Compositions of emeralds from Madagascar. The data are from Hanni and Klein (1982), Gavrilenko et al. (2006) and Vapnik et al. (2006).

cores and deep green rims (Kanis and Schwarz, 2002). According to Cheilletz et al. (2001) the Ianapera deposit may have formed from circulating metamorphic fluids resulting from granulitization and devolatilization of the lower crust due to shearing.

Vapnik et al. (2005) suggested that at the Ianapera deposit the metasomatic process was promoted by fluid migration along the Ampanihy shear zone. They also found that crystals from Ianapera contain the highest reported concentrations of MgO (to 3.95 wt.%), K_2O (to 2.37 wt.%), V_2O_3 (to 0.39 wt.%), Cr_2O_3 (to 4.13 wt.%), and FeO (to 1.82 wt.%) in emeralds. In addition, primary fluid inclusions in the emerald crystals contain heavy hydrocarbons. Vapnik et al. (2005) also found that the crystals formed at the highest pressures and temperatures (630 to 710 °C and 5.0 to 5.8 kbars) yet recorded for emerald.

$^{40}Ar/^{39}Ar$ data from phlogopite returned ages of 490±8 and 493±5 Ma for the Mananjary and Ianapera deposits, respectively (Cheilletz et al., 2001). These dates suggest that both deposits are related to the Pan-African tectono-metamorphic event dated at 500 to 530 Ma (Martelat et al., 2002).

5.13. Mozambique

Emeralds occur in eastern Mozambique near the village of Gité. The two most important deposits are Niame and Rio Maria III (Kanis and Schwarz, 2002). At the Rio Maria III mine the emeralds occur in a biotite–phlogopite–talc schist, which is an alteration product of Precambrian ultramafic rocks. The emeralds often occur with quartz and plagioclase. Other associated minerals include apatite, calcite, fluorite, molybdenite, pyrite, scheelite, and stilbite. Emeralds from Mozambique are typically blue-green in color with many cracks and inclusions (Kanis and Schwarz, 2002).

Vapnik and Moroz (2002) studied fluid inclusions in emeralds from the Maria deposit and reported that they are rich in carbonic acid and that the main daughter phase is nahcolite ($NaHCO_3$), evidence of an alkaline fluid phase. They suggested that the emeralds formed at temperatures of 400 to 500 °C and pressures of 3 to 4 kbar.

5.14. Nigeria

In central Nigeria emerald occurs as a result of early metasomatic albitization of an alkaline granite of the Mesozoic Jos ring complex (Vapnik and Moroz, 2000). The emeralds occur with quartz, feldspar, and topaz in small pegmatitic pockets up to 8 cm in size at the granite-country rock contact, and in small miarolitic pockets in the roof of the granite, in a zone <20 m from the contact with overlying rocks of the Nigerian Basement Complex (Schwarz et al., 1996). The Cr was likely incorporated from the basement schists or younger volcanic rocks (Schwarz et al., 1996). Fluid inclusion data indicate emerald crystallization (of the early and intermediate growth phases) at 400 to 450 °C and 0.2 to 0.3 kbar (Vapnik and Moroz, 2000).

5.15. Norway

Deep green V-dominant emerald occurs at the Byrud Gård mine, 50 km N of Oslo, on the western shore of Lake Mjøsa near Eidsvoll. The emeralds occur where flat-lying nordmarkite-pegmatite dikes and maenaite intrusions (syenite dikes) intrude alum schists. The maximum crystal size is only a few cm (Grundmann and Giuliani, 2002).

5.16. Pakistan

The four main emerald districts in Pakistan are the Swat Valley in the Northwestern Frontier Province, the Malakand and Mohmand areas, the Bajaur Agency, and the Khaltaro area in the Gilgit district (compositions of emerald from the different districts are shown in Fig. 11). The most important is the Swat Valley, approximately 200 km NE of Peshawar. The largest mines are scattered around the NE edge of the town of Mingora. Gujarkili is the second most important mining district in the Swat Valley (Bowersox and Anwar, 1989; Schwarz and Giuliani, 2002c). Giuliani et al. (2000a) used O isotope analysis to show that an emerald in a Gallic–Roman earring originated in the Swat Valley, thus proving that the area has been mined since antiquity. The emeralds in the Swat Valley occur most often with fuchsite and Cr-rich green tourmaline in limonitized shear zones within talc-carbonate rocks traversed by minor quartz veins. The emeralds occur as disseminations and in clusters. In the Swat Valley emeralds also occur with quartz in veins and stockworks within intensely fractured quartz-bearing magnesite rocks, again with fuchsite and Cr-rich tourmaline (Kazmi et al., 1986; Arif et al., 1996). Arif et al. (1996) used stable isotopes to suggest that the mineralization was probably formed by modified hydrothermal solutions derived from an S-type granitic magma. In addition, they proposed that the Swat magnesites formed due to carbonation of previously serpentinized ultramafic rocks by a CO_2-bearing fluid of metamorphic origin.

At the Gandao deposit in the Mohmand area, 40 km NW of Peshawar, V-dominant emeralds occur in quartz veins in a dolomite host (Grundmann and Giuliani, 2002).

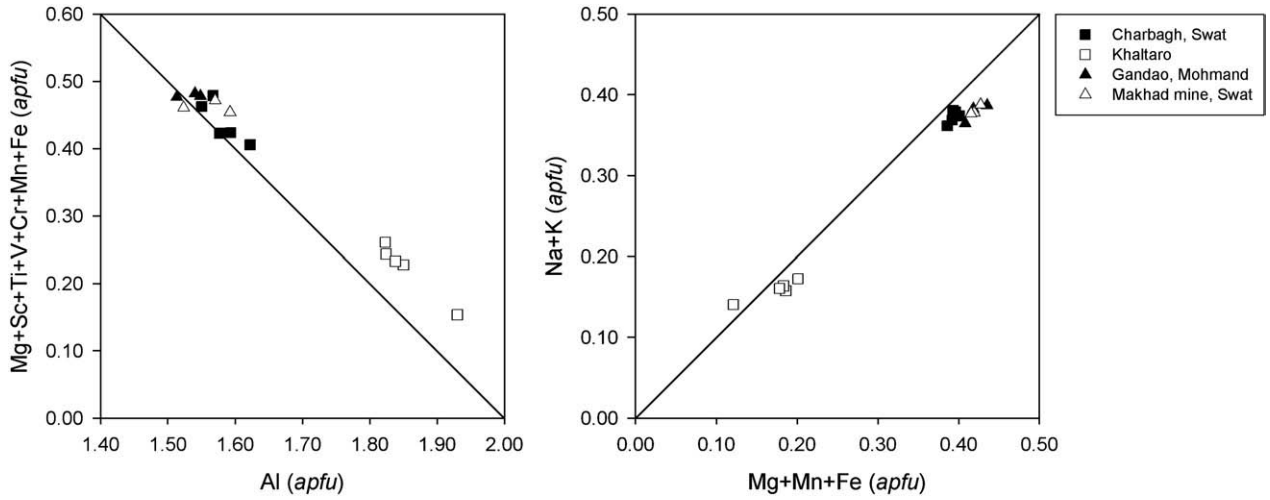

Fig. 11. Compositions of emeralds from Pakistan. The data are from Hammarstrom (1989).

The Khaltaro deposit, approximately 70 km NE of Gilgit in northern Pakistan, was discovered in 1985 by the Gemstone Corporation of Pakistan. At Khaltaro, albite-rich miarolitic pegmatites and hydrothermal veins containing quartz, albite, tourmaline, muscovite, and beryl are associated with a locally albitized leucogranite sill. Pale to medium-green Cr-dominant emeralds up to 3 cm in diameter occur within thin (<0.3 m) quartz and tourmaline-albite veins, and more rarely in pegmatite, near contacts with altered amphibolite (Laurs et al., 1996). The amphibolite is metasomatized in thin selvages (<0.2 m) that are symmetrically zoned around veins or pegmatites. A sporadic inner zone (F-rich biotite, tourmaline, and fluorite, with local albite, muscovite, quartz, and rare beryl) gives way to an intermediate zone (biotite and fluorite and local plagioclase and quartz), which in turn gives way to an outer zone of amphibolite (with sparse biotite and local quartz). The inner and intermediate zones gained H, Li, Be, B, F, K, As, Rb, Sr, Y, Nb, Cs, and Ta, and lost Mg, Si, Ca, Sc, V, Cr, and Fe, and the outer zone gained Li, F, As, Rb, and Cs (Laurs et al., 1996). According to these authors, the emerald formed as a result of HF-rich magmatic-hydrothermal fluids infiltrating the amphibolite at temperatures of 400 to 550 °C, which caused H-ion metasomatism and released Cr and Fe into the pegmatite-vein system. Laurs et al. (1996) pointed out that the Khaltaro deposit is noteworthy because the emerald forms inside of, and not adjacent to, the pegmatite-hydrothermal vein system.

5.17. Russia

The Izumrudnye Kopi emerald district is centered on the Takovaya stream approximately 60 km NE of Ekaterinburg in the Ural Mountains (Grundmann and Giuliani, 2002). The emeralds were discovered in the 1830s; by 1918 the Malyshevsk mine was the world's largest producer of emeralds. Beginning in the 1940's beryllium was produced for nuclear reactors and emeralds were produced as a by-product (3 to 4 million carats in 1950). However, by the mid-1990's mining had virtually ceased. Presently there are four active mines. From N to S, these are Malyshevsk, Sverdlovsk, Cheremshansk, and Krasnobolotnoe. The Malyshevsk deposit accounts for approximately 80% of reserves in the Izumrudnye Kopi district (Gidron, 2007). The current owners (Tsar Emerald Corporation) report that they intend to bring the mine back to its former capacity of 3 million cts per year. The company recently recovered a rough emerald weighing 435 g (approximately 2175 ct; Gidron, 2007).

Kupriyanova (2002) summarized the many previous studies and presented new data on the Izumrudnye Kopi deposits. Intensive granite-related hydrothermal processes in the host ultramafic rocks are associated with a deep fault at the contact between the Murzinsk–Aduisk microcontinent and the Rezhevsk volcanic belt, which is composed of ophiolite sequences. The deposits are within the eastern exocontact of the Aduisk granite pluton (201 to 278 Ma). More than 25 emerald and rare metal (Be, Nb, and Ta) deposits and occurrences (associated with desilicified pegmatites or greisens and albite-microcline pegmatites, respectively) have been identified in the exocontact zone, which is 25 km long and 0.3 to 1.5 km long. These deposits are thought to have formed at deep levels in an environment of intense tectonism. The emerald deposits consist of beryl–quartz–plagioclase veins (which also contain emerald, chrysoberyl ($BeAl_2O_4$), phenakite (Be_2SiO_4) and bromellite (BeO)) and veinlet-metasomatic micaceous zones. The “latitudinal” veins are hosted by dunites, pyroxenites, serpentinites, and rare amphibolites, all of which constitute “hard blocks” with open fractures. The “meridional” veinlet-metasomatic emerald-bearing zones occur between these blocks in “plastic” mylonitic talc schists. Both types of mineralization are associated with the same greisenization event (269–280 Ma). Intensive post-crystallization tectonism altered the initial layering and appearance of the ore bodies, destroyed beryl crystals, and was responsible for the formation of hydrothermal Be-mineral assemblages.

5.18. South Africa

South African emeralds are the world's oldest, at approximately 2.97 Ga. Emeralds have been mined from the Leydsdorp district of the eastern Northern Province (formerly, Northern Transvaal), from the Gravelotte mine in particular, since about 1890. The emeralds are Cr-dominant and attain lengths of 3 cm. The mineralization is associated with albitite pegmatoid bodies which occur along the southern flank of the Archean Murchison Greenstone Belt of the Kapvaal Craton (Robb and Robb, 1986). The emeralds occur in metasomatic “blackwall” zones at the contact between pre-existing pegmatites and biotite-talc and actinolite schists (Grundmann and Morteani, 1989). The pegmatites contain beryl and phenakite. Grundmann and Morteani (1989) suggested a regional metamorphic origin for the emeralds at Leydsdorp (and at Habachtal in Austria) based on the following evidence: (1) augen textures in the metagranitic and metapegmatitic country rocks; (2) sigmoidal inclusion trails in the strongly zoned emeralds, seen as evidence of polystage growth with simultaneous deformation; (3) no evidence for contact metamorphism; and (4) REE fractionation patterns and Yb/Ca versus Tb/Ca ratios for coexisting fluorite crystals

indicate the existence of an abundant non-pegmatitic fluid phase during the formation of the emeralds. Grundmann and Morteani (1989) also suggested the following reactions for the formation of emerald from pre-existing phenakite, based on textural evidence: 3 phenakite + 2 biotite = 2MgFe–beryl + $2K^+$ + 4 Mg^{2+} and 3 phenakite + 3 albite + 2 Mg^{2+} = 2MgNa–beryl + Na^+ + Al^{3+}. Mass balance and geochemical analyses suggested that the transformation of serpentinites and Be-rich country rocks into blackwall zones liberated significant amounts of Be and facilitated the formation of emerald in the presence of Cr.

Nwe and Morteani (1993) studied fluid evolution in the H_2O–CH_4–CO_2–NaCl system during emerald mineralization at the Gravelotte deposit. They identified four types of inclusions. The earliest (Type 1) inclusions, found in phenakites and the emeralds which formed from them, are low salinity (<6 wt.% NaCl) with up to 18 mol% CH_4, and were trapped at 450 to 500 °C and 4 kb. Type 2 fluids reflect mixing of Type 1 fluids with higher salinity brines, and the late Type 3 and 4 inclusions are high salinity (up to 38 wt.% NaCl) with no CH_4 or CO_2. During trapping of the Type 2 inclusions, fluid pressures probably fluctuated due to opening and resealing of fractures. The type 2, 3, and 4 inclusions were trapped at 250, 150, and 240 °C, respectively, and 1 to 4 kb. Calculated low initial fO_2 values were deemed to be uncharacteristic of granitic pegmatite systems, and it was suggested that the phenakites formed in the post-magmatic stage of alkali metasomatism when the albitization took place. In the later stages, phenakite was converted to emerald as the Al activity in the system increased. Metasomatic exchange with the mafic host rocks also increased as evidenced by the incorporation of Cr in the late emeralds. The energy necessary for the continued growth of the later emeralds was probably supplied by regional metamorphism.

Zwaan (2006) questioned some of the arguments used by Grundmann and Morteani (1989) and Nwe and Morteani (1993). He stated that the REE fractionation patterns in fluorite cannot be used to indicate the non-pegmatitic nature of the emerald-forming process because a hydrothermal fluid may be a pegmatite-derived fluid and represent the final stage of magmatic activity. Zwaan (2006) also cited studies of granite–pegmatite systems from the literature to show that the low CO_2 content (seen as evidence that the phenakite did not form magmatically) is not conclusive because the CO_2 content of such systems can often be low. According to Zwaan (2006), the low salinity associated with the formation of phenakite and the initial formation of emerald tends to be related to the later stages of progressive crystallization of granitic magma, and would, therefore, be an argument in favor of a magmatic origin of phenakite and a restriction of early emerald growth to the latest stages of felsic magma crystallization. Zwaan (2006) concluded by stating that although the energy necessary for continued metasomatic exchanges during the various growth phases of the emeralds in the Leydsdorp district might have been supplied by the regional tectono-metamorphic event, a link between pegmatitic activity and the growth of phenakite and (at least early) growth of beryl and emerald should not be ruled out.

5.19. Spain

Emerald was discovered in association with phenakite and gem-quality chrysoberyl in a road-cut at Franqueira in NW Spain in 1968–1969 (Calvo and Garcia, 1997). The chrysoberyl is often cyclic twinned, and many crystals show the alexandrite effect. The geology of the occurrence has been described in detail by Martin-Izard et al. (1992, 1995). The Be minerals occur with apatite in phlogopite-rich zones in a dunite, which was metasomatized by a pegmatite intrusion associated with a two-mica peraluminous granite. Outside of the phlogopite-rich zones the dunite has been altered to tremolite, and there is a narrow anthophyllite zone next to the unaltered dunite. The metasomatic rocks are high in Mg and Cr (from the dunite) and Be, Al, Si, and K (from the pegmatite). The genetic model involves emplacement of pegmatite and associated mobile elements (e.g., Be, B, P) into dunite, with subsequent metasomatism of the dunite to phlogopite-, tremolite-, and anthophyllite-rich schist. Martin-Izard et al. (1995) suggested that because they share structural features the chrysoberyl could have formed by epitactic nucleation on relict olivine crystals. The emerald partially replaces chrysoberyl and phenakite, and could have formed via the reaction chrysoberyl + phenakite + 5quartz → emerald, until the quartz was exhausted (Martin-Izard et al., 1995).

Franz et al. (1996) suggested an alternative genetic model for the Franqueira occurrence. In this model, which was described by Grundmann and Morteani (1989) for the Austrian and South African occurrences, and by Nwe and Morteani (1993) for the South African deposits, a regional multi-stage tectonic and metamorphic event is needed in order for emerald to form at the contact between Be-bearing K–Na–Al–silicate rocks and Cr-rich ultramafic rocks. Martin-Izard et al. (1996) responded that this interpretation was not in accordance with their observations. Their main objection was the assumption by Franz et al. (1996) that the pegmatite-bearing country rocks were thrust onto the granites and that both the granites and pegmatites were metamorphosed. Martin-Izard et al. (1996) presented additional information to show that in their opinion that this was not the case.

Fuertes-Fuente et al. (2000) studied fluid inclusions in emeralds from the Franqueira occurrence and reported that emerald formation took place in the presence of a CO_2- and CH_4-rich fluid at approximately 400 °C and 1 kbar.

5.20. Tanzania

Tanzania's largest emerald deposit is near Mayoka in the northern part of the country, approximately 180 km S of the border with Kenya and 2.5 km W of Lake Manyara. Gem mineralization (emerald, alexandrite, and ruby; Amstutz and Bank, 1977) resulted from high-grade metamorphism and intrusion of pegmatites into basic–ultrabasic rocks (Moroz et al., 2001). The emeralds occur at the contact between pegmatite veins and phlogopite-actinolite schists (Kanis and Schwarz, 2002). Emerald mineralization has been found over a 15 km stretch (Kanis and Schwarz, 2002). The mineralization is structurally controlled by two distinct E-trending strike-slip faults (Kazmi and Snee, 1989). The emerald crystals are dominantly prismatic, rarely exceed 2 cm in length, and range in color from light green to bluish-green.

The Sumbawanga deposit is in western Tanzania about 3 km W of Lake Rukwa. At Sumbawanga the emeralds are found within a weathered basic host penetrated by granitic intrusions (Themelis, 1989). The genesis of the Sumbawanga emeralds is unclear (Moroz et al., 2001).

Pale to dark emerald-green emeralds were discovered in 1994 near Mangola in NW Tanzania, between Lake Eyasi and Ngorongoro Crater (Kanis and Schwarz, 2002).

Moroz et al. (2001) studied solid and fluid inclusions in emeralds from the Mayoka and Sumbawanga deposits. Aragonite, calcite, chrysoberyl, dolomite, magnesite, Mg-rich calcite, nahcolite, and quartz were identified both as mineral inclusions in the emeralds and as trapped solids in the fluid inclusions. The emeralds were estimated to have grown from a carbonic-rich fluid with approximately 6 wt.% NaCl equiv. at temperatures of 370 to 470 °C and pressures of 3.0 to 7.0 kbar. Inclusions of bertrandite, euclase, helvite, and phenakite are common in emeralds from the Sumbawanga deposit. CO_2-rich inclusions with an aqueous phase (usually below detection limit) and $CaCl_2$-rich inclusions with salinities of up to 17 wt.% NaCl equiv. are related to emerald growth. The growth of mineral inclusions predates the trapping of fluid inclusions. The emeralds were estimated to have formed at 220 to 300 °C and 0.7 to 3.0 kbar (Moroz et al., 2001).

5.21. USA

Emerald was discovered in North Carolina, NE of the community of Hiddenite in 1875. Since then a number of notable samples have been discovered, primarily from the Rist and North American Gem mines. Over 3,500 cts of emerald were extracted from the latter in the 1980's, including the 858-ct (uncut) "Empress Caroline" crystal. The Hiddenite emeralds are said to be of a quality comparable to those from Colombia (Wise, 2002).

At the Rist property the emeralds occur in quartz veins and open cavities that occupy NE-trending subvertical fractures in folded metamorphic rocks (Wise and Anderson, 2006). The quartz veins are typically 1 to 10 cm wide and crosscut major folds and all lithologies. Wise and Anderson (2006) identified four cavity assemblages: (1) an emerald-bearing assemblage composed of albite, beryl, calcite, dolomite, muscovite, quartz, rutile, and siderite; (2) a spodumene-bearing assemblage which includes calcite, muscovite, and quartz. The green Cr-bearing spodumene is locally referred to as "hiddenite"; (3) a calcite assemblage dominated by calcite and quartz; and (4) an amethyst assemblage characterized by amethystine quartz, calcite, and muscovite. Emerald and spodumene rarely occur together in the same vein or cavity. Within the emerald-bearing cavities beryl crystals up to 20 cm in length are closely associated with dolomite, muscovite, and quartz. The crystals are typically color-zoned with a pale green to colorless core and an emerald-green rim.

Fluid inclusion studies indicate that mineral precipitation in the cavities occurred as an aqueous-carbonic fluid underwent vapor exsolution between 230 and 290 °C. The presence of abundant open cavities within the quartz veins and evidence of fluid immiscibility suggest that the system evolved under relatively low-pressure conditions (Wise and Anderson, 2006).

Wise and Anderson (2006) point out that the close association of emerald and spodumene within the same quartz vein system clearly distinguishes the Hiddenite occurrences from other emerald deposits. The absence of an evolved pegmatitic phase and the observed mineral assemblages suggest a hydrothermal origin. The source of Be and Cr, and of the Li needed to crystallize spodumene, remains unknown.

Emerald is also found associated with the Crabtree beryl- and tourmaline-bearing pegmatite in the Spruce Pine district of North Carolina. The emerald mineralization occurs in biotite and chlorite schist exocontacts as well as in the discontinuous wall zone of the pegmatite (Tappen, 1998). Aquamarine and yellow beryl also occur in the wall zone, and yellow beryl in the core of the pegmatite. Field observations and compositional data indicate that the yellow beryl crystallized first, followed by green beryl, and then emerald (Tappen, 1998).

Emeralds have also been reported from the Uinta Mountains in Utah, where large veins 0.5 km long and 20 m wide of fibrous, translucent calcite occur in Mississippian carbonates near a fault zone (Keith et al., 1996, 2002; Olcott et al., 1998). Altered zones of Cr-rich (up to 200 ppm) black shale underlie the veins. Three emerald crystals, the largest of which is a 2 cm hexagonal prism weighing 30 ct, have been recovered from the fault zone and shale. The fault zone also contains abundant pyrite, barite, vein quartz, fibrous calcite veins, green mica, and bleached shale (Keith et al., 2002). These authors reported that there is no evidence of igneous activity in the area, and that the isotopic composition of pyrite from the fault zone is similar to that of sulfur from Tertiary oil field brines at the base of the Uinta Basin. Based on these and structural observations, Keith et al. (2002) suggested an origin similar to that of Colombian emeralds. A basinal brine may have mixed with other water along the fault zone or reacted with feldspar and/or dolomite to form emerald and other alteration products. Analyses of C and O isotopes suggested formational temperatures of 200 to 300 °C. Keith et al. (2002) also suggested that, as the sulfate in the brine was reduced by reaction with organic C in the shale, an acidic CO_2-rich fluid was produced, which dissolved parts of the overlying limestone. The fluid may have been neutralized by intermittent loss of CO_2, which led to precipitation of the fibrous calcite (Olcott et al., 1998; Keith et al., 2002).

5.22. Zambia

The Zambian emerald mines are located in the Kafubu area, about 45 km SW of Kitwe in the central part of the country. The emerald deposits are hosted by Cr-rich (3000 to 4000 ppm) talc-chlorite ± actinolite ± magnetite metabasites of the Muva Supergroup, which have been identified as metamorphosed komatiites (Seifert et al., 2004). The metabasite horizons are overlapped by a major field of Be-bearing pegmatites and hydrothermal veins ~10 km in length that was emplaced during the late stages of the Pan African Orogeny (~530 Ma; John et al., 2004). Economic emerald concentrations are almost entirely restricted to phlogopite reaction zones (typically 0.5 to 3 m wide) between quartz-tourmaline veins and the metabasites (Zwaan et al., 2005). Chemical analyses indicate that the formation of phlogopite schists from the metabasite involved the introduction of K_2O (8 to 10 wt.%), F (2.7 to 4.7 wt.%), Li_2O (0.1 to 0.7 wt.%), Rb (1700 to 3000 ppm), Be (up to 1600 ppm), Nb (10 to 56 ppm), and significant amounts of B (Seifert et al., 2004). Information from a fluid inclusion and oxygen isotope study suggested that the veins associated with emerald mineralization formed at 350 to 450 °C and 150 to 450 MPa (Zachariáš et al., 2005). K–Ar dating of muscovite from a pegmatite and an associated quartz-tourmaline vein gave cooling ages of 452 to 447 Ma, which is considered to approximately date the emerald mineralization (Seifert et al., 2004).

5.23. Zimbabwe

Emeralds were discovered in Zimbabwe in 1956 on the southern slope of the Mweza Range, 360 km S of Harare. Today most of the emerald comes from the Sandawana (formerly Zeus) mine which consists of more than 40 km of workings reaching depths of 152 m. Emeralds from the Sandawana mine are known for their bright green color, but cut stones larger than 1.5 ct are rare (Zwaan et al., 1997). They are the oldest commercially available emeralds, having formed around 2.6 Ga. The emerald-forming process was recently described by Zwaan (2006), from whom the following account was adapted. The process began when pegmatites intruded the Mweza Greenstone Belt prior to and/or during a major deformation event. Subsequently, a late-stage Na-rich solution containing Li, Be, F, P, and Cr was injected along shear zones, causing albitization of the pegmatite and phlogopitization of the wallrock. Deformation of the pegmatites, differentiated layering in associated amphibole-phlogopite schist, and (micro) shear zones indicate ductile deformation. The synkinematic growth of emerald, chromian ilmenorutile, fluorapatite, and holmquistite indicates enrichment of Li, Be, F, Na, P, K, Rb, Nb, Cs, and Ta in the shear zones, which suggests that emerald formation is closely related to syntectonic K–Na metasomatism, in which actinolite, albite, cummingtonite, emerald, fluorapatite, holmquistite, and phlogopite crystallized at the expense of microcline, oligoclase, quartz, and chlorite. In addition, mass balance calculations and saline brine inclusions in the emeralds indicate that a Na- and F-rich hydrous fluid was involved in the reactions that ultimately produced emerald. Contact metamorphism is implied by crystallization temperatures of 560 to 650 °C obtained by apatite-phlogopite thermometry, and comparison with what is known about the crystallization paths of pegmatites suggests pressures of 2.3 to 3 kbar (Zwaan, 2006).

Since development of the Sandawana mine, several additional emerald deposits have been identified, most notably the Machingwe mine (12 km NE of the Sandawana mine); this was discovered in 1987 (Kanis et al., 1991).

6. Genetic classification

A number of genetic classification schemes have been proposed for emerald deposits, most recently by Gavrilenko and Dashevsky (1998), Dereppe et al. (2000), Schwarz and Giuliani (2001), Schwarz et al. (2001), Barton and Young (2002), Sabot (2002), and Gavrilenko (2003). Gavrilenko and Dashevsky (1998) and Gavrilenko (2003) studied the gemological and geochemical characteristics of 64 natural and synthetic emeralds from a variety of environments. A number of different techniques including refractometry, specific gravity determinations, luminescence, visible and infrared spectrometry, solid and fluid inclusion studies, and trace element geochemistry were used to separate the natural samples into different groups.

Dereppe et al. (2000) used artificial neural networks (ANN) to classify emerald deposits based on 450 electron microprobe analyses of emeralds from around the world. They defined five categories of deposits: (1) those related to granitic pegmatitic intrusions and hydrothermal veins in mafic-ultramafic rock; (2) those related to tectonism in mafic-ultramafic rocks; (3) those related to oceanic suture zones; (4) those related to thrusts and faults in sedimentary "black shale" rocks; and (5) a "granite-cupola" type (Table 2). The authors reported that classification using ANN data processing gave "bad scores" (misclassifications) of 1, 7, 12.5, 2.6, and 0% for Categories 1 through 5, respectively. The low "classification quality" for Category 3 results from the fact that Afghan emeralds originate from quartz–ankerite–pyrite veins, whereas emeralds from the Swat Valley are found in an (Fe+Mg)-rich environment (talc-carbonate-mica schists) (Dereppe et al., 2000).

Schwarz and Giuliani (2001) and Schwarz et al. (2001) recognized two main types of emerald deposits (Table 3), those related to granitic intrusions (Type 1) and those where mineralization is mainly controlled by tectonic structures, such as thrust faults and shear zones (Type 2). Most emerald deposits fall into the first category and are subdivided on the basis of presence or absence of schist at the contact. Type 2 deposits are subdivided into schists without pegmatites and black shales with veins and breccias.

Zwaan (2006), however, pointed out that a number of emerald deposits cannot be unambiguously classified using this scheme. The Egyptian deposits are classified as schists without pegmatites, but the mineralization is closely related to that of pegmatite veins (Abdalla and Mohamed, 1999). In addition, in the Swat Valley deposits in Pakistan there is a potential link between emerald formation and fluids of pegmatitic origin. These examples suggest that location within major suture or shear zones does not necessarily rule out a connection with granitic intrusions. In addition, Type 1 deposits may have been influenced by tectonism (e.g., Carnaiba, Brazil, and Poona, India). At Leydsdorp in South Africa the emeralds grew syntectonically, but are closely related to pegmatites. This deposit was not classified by Schwarz and Giuliani (2001) or Schwarz et al. (2001).

Barton and Young (2002) divided Be deposits into those with a direct igneous connection and those where such a connection is indirect or absent (i.e., metasomatic). Further subdivision was done on the basis of the associated magma and/or the host rock. Emerald deposits were also grouped by origin (Table 4). Barton and Young (2002) consider the Nigerian deposits to be unusual because they are associated with metaluminous (rather than peraluminous) granitoids. The Swat Valley deposits are classed as carbonate-hosted, but the source of the Cr is the associated ophiolitic melange. For this reason the Swat Valley deposits could be classified as mafic/ultramafic.

Sabot (2002) used the following geological and chemical criteria to classify emerald deposits: (1) oxygen isotope composition; (2) lithium content of the micas; (3) the timing of pegmatite intrusion and emerald formation; (4) the presence of pegmatites and evolved granites and the lack of biotitites and mafic or ultramafic rocks. Based on these data Sabot (2002) proposed the following six classes of emerald deposits: (1) those associated with miarolitic cavities in granites or pegmatites without metasomatic alteration zones (e.g., Kaduna, Nigeria and Emmaville, Australia); (2) deposits in which pegmatites and emeralds are contemporaneous and the latter occur in metasomatic alteration zones in mafic and ultramafic rocks. Tourmaline is present and the lithium content of biotite in the alteration zones exceeds 1000 ppm (e.g., Carnaiba, Brazil, and Kamaganga, Zambia); (3) deposits in which pegmatites and emeralds are contemporaneous and the latter occur in metasomatic alteration zones in mafic and ultramafic rocks. Tourmaline is lacking and the Li content of biotite in the alteration zones is between 100 and 1000 ppm (e.g., Mananjary, Madgascar); (4) no pegmatites contemporaneous with emerald formation but metasomatic alteration zones are present (e.g., Ianapera in Madagascar, the Urals in Russia, and Poona in Australia); (5) no pegmatites and the emeralds occur in carbonate rocks without albite and pyrite (e.g., Swat, Pakistan); and (6) no pegmatites and the emeralds occur in rocks composed of albite and pyrite with evidence of evaporite dissolution (e.g., Colombia).

Table 2
Classification of emeralds by artificial neural networks (Dereppe et al., 2000)

Category	Origin	Examples	"Bad scores" (%)
1	Granitic pegmatite intrusions and hydrothermal veins in mafic-ultramafic rocks	Ndola Rural District, Zambia Sandawana-Machingwe mining area, Zimbabwe Carnaíba-Socotó and Belmont mines-Capoeirana, Brazil Ural Mountains, Russia	1
2	Tectonism (thrusts, shear zones, faults) in mafic-ultramafic rocks	Santa Terezinha and Itaberaí, Goiás State, Brazil	7
3	Oceanic suture zones	Swat Valley, Pakistan Panjsher Valley, Afghanistan	12.5
4	Thrusts and faults in sedimentary "black shale" rocks	Colombia	2.6
5	"Granite-cupola-type"	Kaduna Plateau States, central Nigeria	0

Table 3
Classification scheme of Schwarz and Giuliani (2001) and Schwarz et al. (2001)

Type 1: related to granitic intrusions		Type 2: controlled by tectonic structures	
Pegmatite with schist at contact zone	Pegmatite without schist at contact zone	Schists without pegmatites	Black shales with veins and breccias
Poona, Australia	Emmaville–Torrington, Australia	Panjsher Valley, Afghanistan	Colombia
Bahia (Socoto, Carnaíba), Brazil	Kaduna state, Nigeria	Habachtal, Austria	
Minas Gerais, Brazil	Eidsvoll, Norway	Goiás (Santa Terezinha), Brazil	
Tauá, Brazil		Eastern desert, Egypt	
Tsa da Glisza, Canada		Swat Valley, Pakistan	
Mananjary, Madagascar			
Khaltaro, Pakistan			
Ural Mountains, Russia			
Hiddenite, USA			
Kafubu area, Zambia			
Sandawana, Zimbabwe			

Table 4
Classification scheme of Barton and Young (2002)

Association		Igneous		Metasomatic		
Type	Variety	Magmatic	Pegmatitic	Aluminosilicate (greisen, vein)	Carbonate (skarn, replacement)	Mafic/ultramafic (blackwall, vein)
Direct igneous connection						
Granite	Peraluminous	–	–	–	–	Common; examples: Carnaíba, Brazil; Khaltaro, Pakistan; Reft River, Russia
Indirect or absent ("non-magmatic") igneous connection						
Metamorphic	Shear/vein	–	–	–	Uncommon? Examples: Brumado, Bahia, Brazil; Swat, Pakistan	Uncommon? Example: Habachtal, Austria
Basin	Vein	–	–	Uncommon except in Colombia	–	–

According to Zwaan (2006), the existing classification schemes are ambiguous and not particularly useful when it comes to understanding the mechanisms and conditions that lead to the formation of an emerald deposit. A future classification scheme could be based on trace element geochemistry of the emeralds. For example, in a preliminary study, McManus et al. (2004) used ICP-MS and LIBS (Laser-Induced Breakdown Spectroscopy) to determine the trace element compositions of beryl from pegmatites from different countries. This was done both to understand changes in magmatic and aqueous processes during pegmatite crystallization and to identify source mines to help protect the emerald trade from being used to fund terrorism. Future classification schemes could also be based on stable isotope geochemistry (see below).

7. Stable isotopes

Aines and Rossman (1984) showed that when heated above 400 °C, and after liberation of fluid inclusions, the water in beryl partitions

Table 5
Stable isotope and H_2O data for natural and synthetic emerald (from Giuliani et al., 1997b, 1998; Groat et al., 2002)

Country	Locality or source	δ18O (‰ SMOW)	δD channel (‰ SMOW)	H_2O channel (wt.%)*	Country	Locality or source	δ18O (‰ SMOW)	δD channel (‰ SMOW)	H_2O channel (wt.%)*
Afghanistan	Kendjt	13.6	−45.5	1.93			18.7	−18.9	1.61
	Khalat-1	13.35	−45.5	2.04		Penas Blancas	19.7	−8.4	1.96
	Gujari	13.25	−47.8	2.17		Repolal	18.7	−23.8	1.31
	Shabaki	13.9	−45.8	2.05		Tequendama	21.95	−28.6	1.89
Australia	Emmaville	11.2	−83.4	0.87		Yacopi	21.4	−19.2	1.89
	Menzies	9.0	−42.3	1.98			21.5	−22.2	1.80
	Poona	7.0	−43.8	2.49	Egypt	Sikait	10.3	−54.6	3.13
	Torrington	9.9	−89.0	0.83			10.5	−61.0	2.77
Austria	Habachtal	7.3	−21.1	3.33			10.4	−62.2	
		7.2	−23.0	2.92	India	Rajasthan	10.8	−43.4	2.57
		6.9	−24.4	2.95	Madagascar	Morafeno	9.4	−35.8	2.65
Brazil	Capoeirana	6.3	−40.0	2.57			8.5	−27.3	
	Carnaíba	9.6	−53.7	2.47	Mozambique	Maria	8.2	−47.0	2.25
	Coqui	12.1	−41.3	2.40	Nigeria	Kaduna	9.9	−50.7	0.97
	Itaberai	12.1	−35.4	3.16			9.4	−43.3	0.89
	Juca	6.8	−35.5	1.23			9.7	−52.7	0.94
	Pela Ema	11.8	−34.8	2.88	Norway	Mjosa-See	9.4	−40.8	1.10
	Pirenópolis	9.4	−28	3.01			9.6	−37.8	1.10
	Pombos	7.5	−28.1	2.78	Pakistan	Khaltaro	10.6	−87.7	2.12
	Santa Terezinha	12.4	−36.1	3.13		Swat	15.4	−51	
		12.0	−29.8	2.90			15.8	−48	
		12.4	−30.0	2.95			15.1	−42	
		12.1	−34.0	3.00			15.9	−32	
	Socotó	10.9	−41.0	2.53			15.4	−37	
Bulgaria	Rila	9.5	−30.2	1.95			15.7	−44	
		9.4	−29.8	2.40			16.2	−39	
		9.3	−32.7	2.21	Russia	Malyshevsk	10.2	−40.8	2.83
Canada	Tsa da Glisza	14.0	−59.8	2.07			11.0	−40.7	2.35
		13.3	−57.3	1.91	South Africa	Leydsdorp	9.5	−25.3	2.45
Colombia	El Pulpito	17.4	−27.9	1.31			9.7	−33.1	2.30
Eastern Zone	Guala	16.8	−21.9	1.37	Spain	Franqueira	9.75	−23.3	2.30
	Guali	16.65	−11.0	1.62					
	Klein	17.2	−20.3	1.50	Tanzania	Sumbawanga	11.7	−41.3	0.84
		17.2	−23.2	1.55	Zambia	Miku	9.8	−41.6	2.75
	Oriente	18.3	−28.6	1.39			10.4	−35.0	2.70
		18.3	−27.0	1.32	Zimbabwe	Sandawana	8.0	−53.3	2.30
	Palo Aranado	17.1	−15.5	1.34			6.9	−25.0	2.80
		17.1	−8.7	1.26					
	Vega	18.1	−7.1	1.33	Australia	Biron	−5.0	−80.5	1.31
Colombia	Cincho	22.7	−18.2	1.63	Russia	Bidulite (1997)	−9.0	−95.4	1.53
Western Zone		22.7	−15.0	1.55	Russia	Bukin	−0.9	−109.3	1.16
	Coscuez	24.75	−17.7	1.94	Russia	Krasnoïarsk	−6.3	−104.8	1.03
	Guaquimay	21.1	−27.2	1.64	Russia	Tairus (1997)	−2.1	−114.2	1.19
	Pava	18.7	−25.7	1.44	USA	Regency (1983)	−1.6		

*Or H_2O^+.

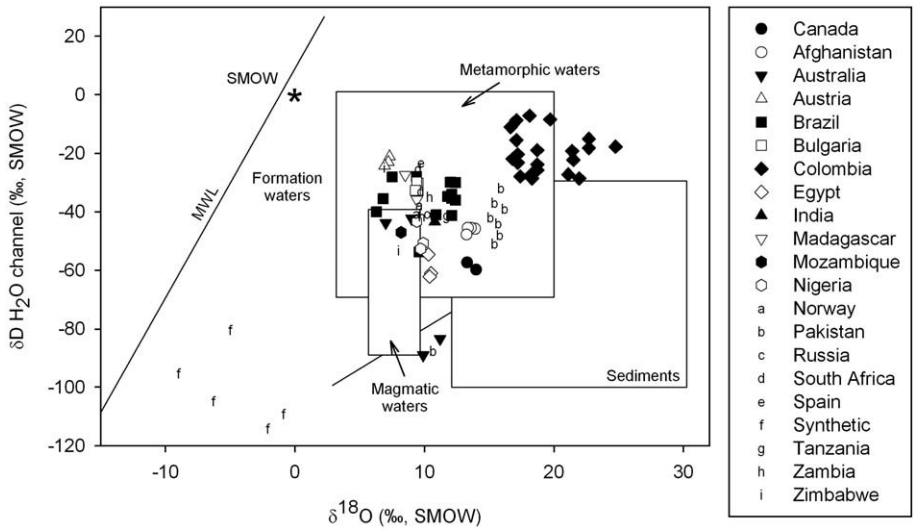

Fig. 12. Channel δD H_2O vs. $\delta^{18}O$ (‰, SMOW, standard mean ocean water) for natural emeralds from a number of world localities and synthetic hydrothermal emeralds. The data are from Fallick and Barros (1987), Arif et al. (1996), Giuliani et al. (1997a, 1998), Groat et al. (2002), and our own unpublished studies. The isotopic compositional fields are from Sheppard (1986). MWL = Meteoric Water Line.

into an unbound state as gaseous molecules confined to the channel voids. Brown and Mills (1986) showed that the channel H_2O is liberated at temperatures of ~800 °C, and Taylor et al. (1992) reported that isotopic fractionation seems to be minimal during dehydration. Thus, channel H_2O may represent the original fluid composition from the time of formation, and the measurement of δD in H_2O released from beryl may then permit determination of the source of the fluids from which the beryl grew. Such investigations have been applied successfully to beryl from a number of deposits (Fallick and Barros, 1987; Taylor et al., 1992; Arif et al., 1996; Giuliani et al., 1997a,b, 1998, 2000b). In addition, Giuliani et al. (2000a) used isotopic compositions of historical emerald artifacts to show that during historical times artisans worked with emeralds originating from deposits supposedly discovered in the 20th Century, and that most of the high-quality emeralds cut in the 18th Century in India originated from Colombia. Table 5 reports hydrogen and oxygen isotopic compositions for emeralds from a number of world localities and synthetic hydrothermal emeralds, and these data are shown in Fig. 12. Table 6 and

Table 6
Stable isotope and fluid inclusion data for natural emeralds

Country	Locality	Average $\delta^{18}O$ emerald (‰)	Average δD channel (‰)	Temperature of emerald formation (°C)	Calculated $\delta^{18}O$ H_2O LT	Calculated $\delta^{18}O$ H_2O HT	Fluid inclusions references
Afghanistan	Panjshir	13.5(3)	−46.2(3)	200–350	10.33	12.99	Seal (1989)
				300–400§	12.34	13.5	Vapnik and Moroz (2000)
Austria	Habachtal	7.1(2)	−23.0(1.0)	500–550§	7.81	8.08	Nwe and Grundmann (1990)
Brazil	Coqui	12.1	−41.3*	250–300	10.09	10.94	Cheilletz et al. (1991)
	Capoeirana	6.2(1)	−40.0*	450–650§	6.59	7.57	De Souza et al. (1992)
	Carnaíba	9.05(1)	−53.7*	300–350	7.89	8.54	Giuliani et al. (1997a)
	Socotó	10.9	−41.0*	300–350	9.74	10.39	Giuliani et al. (1997a)
	Porangatu	11.0(3)†	−40.0(5.0)†	350–630§	10.49	12.3	Barros and Kinnaird (1985), Cassedanne and Barros (1986)
	S. Terezinha	12.2(1)	−33.0(3.1)*	330–490	11.45	12.86	Giuliani et al. (1997a)
Bulgaria	Rila	9.4(1)	−31.0(1.0)	300–400	8.24	9.4	Alexandrov et al. (2001)
Canada	Tsa da Glisza	13.3(10)	−57.3(2.2)	260–340	11.48	12.67	Groat et al. (2002)
		14.0(7)	−59.8(2.2)	260–340	12.18	13.37	Groat et al. (2002)
Colombia	Eastern zone	17.4(6)	−19.1(7.7)*	260–340§	15.58	16.77	Giuliani et al. (1992)
	Western zone	21.1(1.9)	−20.4(5.6)*	300–320§	19.94	20.22	Cheilletz et al. (1994)
				325	20.29	20.29	Ottaway et al. (1994)
Egypt	Sikait	10.4(1.0)	−59.0(3.0)	260–380	8.58	10.21	Abdalla and Mohamed (1999)
Nigeria	Kaduna	9.7(2.0)	−49.0(4.0)	400–450	9.7	10.09	Vapnik and Moroz (2000)
Pakistan	Khaltaro	10.65(10)	−87.7	400–550§	10.65	11.63	Laurs et al. (1996)
	Swat	15.6(3)	−41.9(5.6)‡	380–450§	15.41	15.99	Seal (1989)
Russia	Malyshevsk	10.6(4)	−40.8(1.0)	270–280	8.96	9.13	Moroz and Vapnik (1999)
S. Africa	Leydsdorp	9.6(1)	−29.0(4.0)	450–500§	9.99	10.31	Nwe and Morteani (1993)
Spain	Franqueira	9.8	−23.3	320–380§	8.92	9.61	Martin-Izard et al. (1995)
Tanzania	Sumbawanga	11.7	−41.3	380–400	11.51	11.7	Moroz and Vapnik (1999)
Zambia	Miku	10.1(3)	−38.0(3.0)	240	7.88	7.88	Moroz and Vapnik (1999)

Hydrogen-isotope composition of water from channels (δD channel) was obtained on the same samples studied for the oxygen-isotope composition of emerald ($\delta^{18}O$) and published in Giuliani et al. (1998). δD data references: * = Giuliani et al. (1997b). The δD values for the Colombian emeralds are average values (Eastern emerald zone, n = 7 deposits; western emerald zone, n = 8 deposits); † = Fallick and Barros (1987); ‡ = from Arif et al. (1996). Fluid-inclusions and temperature of emerald formation: § = trapping temperature; without symbols = minimum trapping temperature (range of homogenisation temperatures).

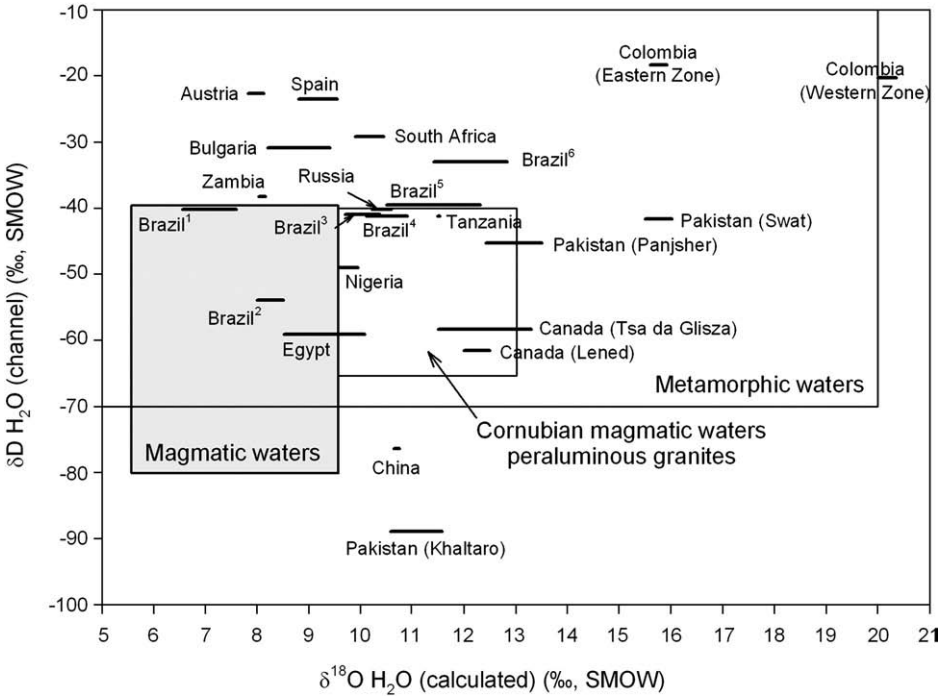

Fig. 13. Average channel δD H_2O vs. calculated $\delta^{18}O$ for water in equilibrium with beryl at a given temperature (‰, SMOW, standard mean ocean water) for emeralds from a number of world localities (Brazil[1] = Capoeirana, 2 = Carnaiba, 3 = Socoto, 4 = Coqui, 5 = Porangatu, and 6 = Santa Terezinha). The equation used to calculate oxygen fractionation between beryl and water is from Taylor et al. (1992): $10^3 \ln \alpha_{\text{beryl–water (250–500 °C)}} = 1.579(10^6/T^2) - 0.645(10^3/T) - 2.522$ (T = temperature in Kelvin). Sources of data are the same as in Fig. 12. Temperatures, which were derived from fluid inclusion data, are from the following studies: Barros and Kinnaird (1985), Cassedanne and Barros (1986), Seal (1989), Nwe and Grundmann (1990), Cheilletz et al. (1991, 1994), De Souza et al. (1992), Giuliani et al. (1992, 1997b), Nwe and Morteani (1993), Ottaway et al. (1994), Martin-Izard et al. (1995), Abdalla and Mohamed (1999), Moroz and Vapnik (1999), Vapnik and Moroz (2000), Groat et al. (2002), and our own unpublished work. The isotopic compositional fields are from Sheppard (1986).

Fig. 13 show average hydrogen isotopic compositions versus oxygen isotopic compositions for water in equilibrium with beryl calculated using temperatures derived from fluid inclusion data.

8. Exploration

Emerald may be identified in the field by color, hardness (7.5–8), and form (hexagonal prisms with pinacoids). When viewed through a Chelsea filter emerald is red, but note that other Cr-bearing green gems may show the same reaction.

Simandl et al. (1999a,b) and Walton (2004) provide summaries and exploration guides for the different types of emerald deposits. For example, chrysoberyl and phenakite are obvious indicator minerals for metamorphic-type occurrences. It may also be instructive to review some of the publications associated with recent emerald exploration in NW Canada. Murphy et al. (2002) plotted potential Be reservoirs (plutonic rocks) and Cr and V reservoirs (ultramafic rocks, volcanic rocks, and the Earn Group black shales) in the Yukon Territory and suggested that the best place to look is where the two come together. Goodfellow and Aronoff (1988) used Landsat imagery and surficial geochemical data to search for buried, and hence overlooked, plutons in the western Northwest Territories; this might be a good approach for other regions as well. Lewis et al. (2003) noted that all beryl occurrences in the Yukon Territory are intrusion-related, but for an intrusion to become enriched enough to reach Be-saturation to form beryl it must be "ultrafractionated". Numerous lithological and geochemical features (e.g., accessory mineralogy, Rb/Sr ratio from whole rock compositions, K/Rb ratio in potassic feldspar, and others) can help pinpoint fractionated pegmatites with elevated gemstone potential.

Companies exploring for emerald in NW Canada have been relying heavily on Be and Cr analyses of stream-sediment and soil samples. Commercial analyses utilizing rapid single-stage digestion techniques may not adequately dissolve the refractory mineral phases that typically incorporate Be and Cr (Groat et al., 2005). In addition, the use of mass spectrometry to analyse Be, which is an extremely light element, in an analytical package that includes numerous heavy elements, may decreases the sensitivity of the Be analyses (Groat et al., 2005).

Geochemistry has proven to be useful in Colombia. Escobar (1978) studied the geology and geochemistry of the Gachalá area and found that Na enrichment and depletion of Li, K, Be, and Mo in the host rocks were very good indicators for locating mineralized areas. Beus (1979) presented the results of a United Nations-sponsored geochemical survey of the streams draining emerald deposits in the Chivor and Muzo areas. The spatial distribution of areas with emerald mineralization was linked, on a regional scale, to intersections of the NNE and NW trending fault zones. The black shales in those tectonic blocks which contain emerald mineralization were found to be enriched in CO_2, Ca, Mg, Mn, and Na, and depleted in K, Si, and Al (Beus, 1979). The results of this study were tested with a stream sediment sampling program in the Muzo area. The results showed that samples collected from emerald-bearing tectonic blocks had anomalously low K/Na ratios. Subsequently it was discovered that the Na content of the sediments was the best indicator of the mineralized zones in the drainage basins. Several new emerald occurrences were discovered by U.N. teams using the results of this study.

More recently, Ringsrud (1986) reported that Colombian geologists were analyzing soil samples collected from altered tectonic blocks for Li, Na, and Pb to delineate emerald mineralization. Cheilletz et al. (1994) showed that the Be content of black shales outside of the leached mineralized areas ranges from 3.4 to 4 ppm. Beryllium concentrations in the leached areas were found to range from 0.1 to 3.0 ppm (Beus, 1979).

Structural geology is also important for emerald exploration in Colombia (Branquet et al., 1999a,b). In the western zone (Muzo and Coscuez areas), deposits are linked by tear faults and associated thrusts. The thrust geometry is linked to decollement planes. The

difficulty resides in the hectometric scale of the mineralized structures which represent disharmonies in large anticlinorium (Branquet et al., 1999b).

Laskovenkov and Zhernakov (1995) reported that berylometers, instruments that use Sb^{124}-sourced gamma radiation to excite a response from Be atoms, can used to locate emerald occurrences by mapping the Be content of the host rocks. At least two models are commercially available. The most portable unit weighs 2 kg, but requires counting times of 2–5 min, and has a lower detection limit of only 0.01% BeO. The second model requires counting times of 1–2 min and has a lower detection limit of 0.003% BeO, but weighs 17 kg. The weights, counting times, and detection limits confine their application to property studies.

It is important to note that exploration for gem beryl could result in the discovery of new occurrences of non-gem beryl or other Be minerals that could become new sources of Be and Be oxide. Most Be is used as an alloy, metal, or oxide in electronic and electrical components and aerospace and defence applications. About 60% of world production is from bertrandite [$Be_4Si_2O_7(OH)_2$] ore mined from an epithermal deposit at Spor Mountain in Utah (Cunningham, 2004). Granite-focused exploration could also result in the discovery of other commodities, such as Au, Ag, and W.

9. Future research

It became apparent as we were preparing this study that there is a paucity of modern electron microprobe and trace element compositions for emerald. A comprehensive library of such compositions would be a valuable asset to future researchers. As noted above the role of metamorphism in the formation of some emerald deposits (notably Habachtal in Austria, Leydsdorp in South Africa, and Franqueira in Spain) is controversial and thus worthy of additional study. As suggested by Zwaan (2006), there is a need for an unambiguous classification scheme that would aid in our understanding of the mechanisms and conditions that lead to the formation of emerald deposits. Finally, further development of exploration guidelines for emerald would be desirable.

Acknowledgements

The authors thank Mackenzie Parker for editing the manuscript, and Allison Brand and Brad Wilson for help with the References. The manuscript was improved by comments from an anonymous reviewer, J.C. Zwaan, Associate Editor Ian Graham, and the Editor Nigel Cook.

References

Abdalla, H.M., Mohamed, F.H., 1999. Mineralogical and geochemical investigation of emerald and beryl mineralisation, Pan-African Belt of Egypt: genetic and exploration aspects. Journal of African Earth Sciences 28, 581–598.

Aines, R.D., Rossman, G.R., 1984. The high-temperature behavior of water and carbon dioxide in cordierite and beryl. American Mineralogist 69, 319–327.

Alexandrov, P., Guiliani, G., Zimmerman, J.L., 2001. Mineralogy, age and fluid geochemistry of the Rila Emerald deposits, Bulgaria. Economic Geology 96, 1469–1476.

Amstutz, G.C., Bank, H., 1977. Geologische, petrographische und mineralogische Beobachtungen in einigen Minen von Smaragd, Transanit und Rubin in Tansania und Kenya. Zeitschrift Deutschen Gemmologischen Gesellschaft 26, 118–127.

Arif, M., Fallick, A.E., Moon, A.E., 1996. The genesis of emeralds and their host rocks from Swat, northwestern Pakistan: a stable-isotope investigation. Mineralium Deposita 31, 255–268.

Artioli, G., Rinaldi, R., Stahl, K., Zanazzi, P.F., 1993. Structure refinements of beryl by single-crystal neutron and X-ray diffraction. American Mineralogist 78, 762–768.

Barros, J.C., Kinnaird, J.A., 1985. Fluid inclusion studies of emeralds and green beryls from the Porangatu deposit, Goiás state, Brazil. Proceedings of the VIII European current research on fluid inclusions (ECROFI).

Barton, M.D., Young, S., 2002. Non-pegmatitic deposits of beryllium: mineralogy, geology, phase equilibria and origin. In: Grew, E.S. (Ed.), Beryllium: Mineralogy, Petrology, and Geochemistry. Reviews in Mineralogy and Geochemistry, vol. 50, pp. 591–691.

Basta, E.Z., Zaki, M., 1961. Geology and mineralisation of Wadi Sikeit area, South-Eastern Desert. Journal of Geology of the United Arab Republic 5, 1–36.

Beus, A.A., 1979. Sodium — a geochemical indicator of emerald mineralization in the Cordillera Oriental, Colombia. Journal of Geochemical Exploration 11, 195–208.

Beus, A.A., Mineev, D.A., 1972. Some Geological and Geochemical Features of the Muzo-Coscuez Emerald Zone, Cordillera Oriental, Colombia. Empresa Colombiana de Minas, Biblioteca, 55 pp. (unpubl.).

Blauwet, D., Quinn, E.P., Muhlmeister, S., 2005. New emerald deposit in Xinjiang, China. Gems and Gemology 41, 56–57.

Bowersox, G.W., Anwar, J., 1989. The Gujar Killi emerald deposit, Northwest Fronteir Province, Pakistan. Gems and Gemology 25, 16–24.

Bowersox, G.W., Snee, L.W., Foord, E.F., Seal II, R.R., 1991. Emeralds of the Panjshir Valley, Afghanistan. Gems and Gemology 27, 26–39.

Brand, A.A., 2006. Cr-dominant emerald mineralization associated with pegmatitic granite at Dryden, Ontario. Unpublished B.Sc. thesis, University of British Columbia, Vancouver, BC, Canada. 52 pp.

Branquet, Y., Laumonier, B., Cheilletz, A., Giuliani, G., 1999a. Emeralds in the Eastern Cordillera of Colombia: two tectonic settings for one mineralization. Geology 27, 597–600.

Branquet, Y., Cheilletz, A., Giuliani, G., Laumonier, B., 1999b. Fluidized hydrothermal breccia in dilatant faults during thrusting: the Colombian emerald deposits. In: McCaffrey, K.J.W., Lonergan, L., Wilkinson, J.J. (Eds.), Fractures, Fluid Flow and Mineralization, vol. 155. Geological Society of London, pp. 183–195. Special Publication.

Brown Jr., G.E., Mills, B.A., 1986. High-temperature structure and crystal chemistry of hydrous alkali-rich beryl from the Harding pegmatite, Taos County, New Mexico. American Mineralogist 71, 547–556.

Calligaro, T., Dran, J.C., Poirot, J.P., Querré, G., Salomon, J., Zwaan, J.C., 2000. PIXE/PIGE characterization of emeralds using an external micro-beam. Nuclear Instruments and Methods in Physics Research B 161–163, 769–774.

Calvo, M., Garcia, J.R., 1997. Emerald and associated minerals from A Franqueira, Pontevedra, Spain. Mineralogical Record 28, 497–501.

Cassedanne, J.P., Barros, J.C., 1986. Quelques gites d'emeraude de Goias. Revue de Gemmologie A.F.G. 88, 9–12.

Cassedanne, J.P., Cassedanne, J.O., Mello, Z.F., 1979. As esmeraldas de Tauá e Pilão Arcado. Mineração Metalurgica 410, 50–58.

Cheilletz, A., Féraud, G., Giuliani, G., Rodriguez, C.T., 1991. $^{40}Ar/^{39}Ar$ laser-probe dating of the Colombian emerald deposits; metallogenic implications. In: Pagel, M., Leroy, J. (Eds.), Source, Transport and Deposition of Metals. Balkema, Rotterdam, pp. 373–376.

Cheilletz, A., Féraud, G., Giuliani, G., Rodriguez, C.T., 1994. Time-pressure and temperature constraints on the formation of Colombian emeralds: An $^{40}Ar/^{39}Ar$ laser microprobe and fluid inclusion study. Economic Geology 89, 361–380.

Cheilletz, A., Giuliani, G., Branquet, Y., Laumonier, B., Sanchez, A.J.M., Féraud, G., Arhan, T., 1997. Datation K–Ar et $^{40}Ar/^{39}Ar$ à 65±3 Ma des gisements d'émeraude du district de Chivor–Macanal: argument en faveur d'une déformation précoce dans la Cordillère Orientale de Colombie. Comptes Rendus de l'Académie des Sciences, Paris 324, 369–377.

Cheilletz, A., Sabot, B., Marchand, P., De Donato, P., Taylor, B., Archibald, D., Barres, O., Andrianjaffy, J., 2001. Emerald deposits in Madagascar: two different types for one mineralizing event. European Union of Geosciences. Journal of Conference Abstracts 6, 547.

Chielletz, A., Giuliani, G., 1996. The genesis of Colombian emeralds: a restatement. Mineralium Deposita 31, 359–364.

Conklin, L.H., 2002. What is emerald — fact and opinion. ExtraLapis English 2, 72–73.

Couto, P.A., Sampaio, A.R., Gil, C.A.A., Loureiro, H.C., Arcanjo, J.B., Fernandes Filho, J.F., Guimarães, J.T., Melo, R.C., 1978. Projeto Serra da Jacobina: geologia e prospecção geoquimíca. Relatório final, Convênio DNPN/CPRM, Salvador da Bahia.

Cunningham, L.D., 2004. Beryllium. U.S. Geological Survey, Mineral Commodity Summaries, January 2004, pp. 32–33.

De Souza, J.L., Mendes, J.C., Da Silveira Bello, R.M., Svisero, D.P., Valarelli, J.V., 1992. Petrographic and microthermometrical studies of emeralds in the "Garimpo" of Capoerana, Nova Era, Minas Gerais State, Brazil. Mineralium Deposita 27, 161–168.

Dereppe, J.M., Moreaux, C., Chauvaux, B., Schwarz, D., 2000. Classification of emeralds by artificial neural networks. Journal of Gemmology 27, 93–105.

Dilles, J.H., Snee, L.W., Laurs, B.M., 1994. Geology, Ar–Ar age and stable isotope geochemistry of suture-related emerald mineralization, Swat, Pakistan Himalayas. Geological Society of America, Abstracts with Programs 26, 311.

Escobar, R., 1978. Geology and geochemical expression of the Gachala emerald district, Colombia. Geological Society of America, Abstracts with Programs 10, 397.

Escobar, R., Mariano, A.N., 1981. On the origin of the Colombian emeralds. Nuclide Spectra XIV, 1025/1081.

Fallick, A.E., Barros, J.G., 1987. A stable-isotope investigation into the origin of beryl and emerald from the Porangatu deposits, Goiás state, Brazil. Isotope Geoscience 66, 293–300.

Feng, M., Lu, W., Zhang, X., Chen, G., Zhang, S., 1998. Regional geologic mapping report for Malipo and Dulong sheet at 1:50,000. Yunnan Bureau of Geology and Exploration, internal publication.

Fijal, J., Heflik, W., Natkaniec-Nowak, L., Szczepaniak, A., 2004. Emeralds from the Panjshir Valley (Afghanistan). Gemmologie: Zeitschrift der Deutschen Gemmologischen Gesellschaft 53, 127–142.

Franz, G., Morteani, G., 2002. Be-minerals: synthesis, stability, and occurrence in metamorphic rocks. In: Grew, E.S. (Ed.), Beryllium: Mineralogy, Petrology and Geochemistry. Reviews in Mineralogy and Geochemistry, vol. 50, pp. 551–589.

Franz, G., Gilg, H.A., Grundmann, G., Morteani, G., 1996. Metasomatism at a granitic pegmatite–dunite contact in Galicia: the Franqueira occurrence of chrysoberyl

(alexandrite), emerald, and phenakite: discussion. Canadian Mineralogist 34, 1329–1331.
Fuertes-Fuente, M., Martin-Izard, A., Boiron, M.C., Viñuela, J.M., 2000. P–T path and fluid evolution in the Franqueira granitic pegmatite, central Galicia, Northwestern Spain. Canadian Mineralogist 38, 1163–1175.
Garland, M.I., 2004. The Dryden Emerald Occurrence, Taylor pegmatite, Zealand Township, NW Ontario. True North Gems Inc., unpublished internal company report.
Garstone, J.D., 1981. The geological setting and origin of emeralds from Menzies, Western Australia. Journal of the Royal Society of Western Australia 64, 53–64.
Gavrilenko, E.V., 2003. Esmeraldas de los Urales (Rusia): condiciones de formacion y caracterizacion comparativa con las esmeraldas de otros origenes. Unpublished M. Sc. thesis, Universidad Politécnica de Madrid, Spain. 330 pp.
Gavrilenko, E.V., Dashevsky, D.M., 1998. Properties of emeralds of different genesis and their diagnostic meaning. Proceedings of the Russian Mineralogical Society 127, 45–57 (in Russian).
Gavrilenko, E.V., Pérez, B.C., 1999. Characterisation of emeralds from the Delbegetey deposit, Kazakhstan. In: Stanley, C.J., et al. (Ed.), Mineral Deposits: Processes to Processing. Balkema, Rotterdam, pp. 1097–1100.
Gavrilenko, E.V., Pérez, B.C., Bolibar, R., Castroviejo Garcia del Amo, D., 2006. Emeralds from the Delbegetey deposit (Kazakhstan): mineralogical characteristics and fluid-inclusion study. Mineralogical Magazine 70, 159–173.
Gidron, M.J., 2007. Russia's Malyshev emerald mine reopens under new management. InColor 21–22 Spring 2007.
Giuliani, G., Silva, L.J.H.D., Couto, P., 1990. Origin of emerald deposits of Brazil. Mineralium Deposita 25, 57–64.
Giuliani, G., Sheppard, S.M.F., Cheilletz, A., Rodriguez, C., 1992. Contribution de l'étude des phases fluides et de la géochimie isotopique $^{18}O/^{16}O$, $^{13}C/^{12}C$ à la genèse des gisements d'émeraude de la Cordillère orientale de la Colombie. Comptes Rendus de l'Académie des Sciences, Paris 314, 269–274.
Giuliani, G., Cheilletz, A., Arboleda, C., Carrillo, V., Rueda, F., Baker, J.H., 1995. An evaporitic origin of the parent brines of Colombian emeralds: fluid inclusion and sulphur isotope evidence. European Journal of Mineralogy 7, 151–165.
Giuliani, G., France-Lanord, C., Zimmermann, J.L., Cheilletz, A., Arboleda, C., Charoy, B., Coget, P., Fontan, F., Giard, D., 1997a. Fluid composition, dD of channel H_2O, and $d^{18}O$ of lattice oxygen in beryls: genetic implications for Brazilian, Colombian, and Afghanistani emerald deposits. International Geology Review 39, 400–424.
Giuliani, G., Cheilletz, A., Zimmermann, J.L., Ribeiro-Althoff, A.M., France-Lanord, C., Feraud, G., 1997b. Les gisements d'émeraude du Brésil: genèse et typologie. Chronique de la Recherche Minière 526, 17–61.
Giuliani, G., France-Lanord, C., Coget, P., Schwarz, D., Cheilletz, A., Branquet, Y., Giard, D., Martin-Izard, A., Alexandrov, P., Piat, D.H., 1998. Oxygen isotope systematics of emerald: relevance of its origin and geological significance. Mineralium Deposita 31, 513–519.
Giuliani, G., Bourles, D., Massot, J., Siame, L., 1999. Colombian emerald reserves inferred from leached beryllium of their host black shale. Exploration and Mining Geology 8, 109–116.
Giuliani, G., Chaussidon, M., Schubnel, H.-J., Piat, D.H., Rollion-Bard, C., France-Lanord, C., Giard, D., de Narvaez, D., Rondeau, B., 2000a. Oxygen isotopes and emerald trade routes since antiquity. Science 287, 631–633.
Giuliani, G., Christian, F., Cheilletz, A., Coget, P., Branquet, Y., Laumomnier, B., 2000b. Sulfate reduction by organic matter in Colombian emerald deposits: chemical and stable isotope (C,O, H) evidence. Economic Geology 95, 1129–1153.
Giuliani, G., Marty, B., Banks, D., 2005. Noble gases in fluid inclusions from emeralds: implications for the origin of fluids and constraints on fluid-rock interactions. Proceedings of the XVIII European current research on fluid inclusions (ECROFI).
Glover, J.K., Burson, M.J., 1987. Geology of the Lened tungsten skarn deposit, Logan Mountains, Northwest Territories. In: Morin, J.A. (Ed.), Mineral Deposits of the Northern Cordillera Special Volume, vol. 37. Canadian Institute of Mining and Metallurgy, pp. 255–265.
Goodfellow, W.D., Aronoff, S., 1988. Application of Landsat imagery and surficial geochemistry to the discovery of tungsten skarn deposits associated with buried plutons. Geocarto International 3, 3–16.
Govorov, J.N., Stunzhas, A.A., 1963. On the forms of beryllium transport in alkaline metasomatose. Geokhimiya 4, 383–390.
Graziani, G., Gübelin, E., Lucchesi, S., 1983. The genesis of an emerald from the Kitwe District, Zambia. Neues Jahrbuch für Mineralogie Monatshefte 175–186.
Groat, L.A., Marshall, D.D., Giuliani, G., Murphy, D.C., Piercey, S.J., Jambor, J.L., Mortensen, J.K., Ercit, T.S., Gault, R.A., Mattey, D.P., Schwartz, D.P., Maluski, H., Wise, M.A., Wengzynowski, W., Eaton, W.D., 2002. Mineralogical and geochemical study of the Regal Ridge emerald showing, southeastern Yukon. Canadian Mineralogist 40, 1313–1338.
Groat, L.A., Hart, C.J.R., Lewis, L.L., Neufeld, H.L.D., 2005. Emerald and aquamarine mineralization in Canada. Geoscience Canada 32, 65–76.
Grundmann, G., Giuliani, G., 2002. Emeralds of the world. ExtraLapis English 2, 24–35.
Grundmann, G., Morteani, G., 1989. Emerald mineralisation during regional metamorphism: the Habachtal (Austria) and Leydsdorp (Transvaal, South Africa) deposits. Economic Geology 84, 1835–1849.
Grundmann, G., Morteani, G., 1993. Emerald formation during regional metamorphism: the Zabara, Sikeit and Um Kabu deposits (Eastern Desert, Egypt). International Conference on Geoscientific Research in Northeast Africa, Proceedings, pp. 495–498.
Grundmann, G., Morteani, G., 1995. Australia Ein neues Vorkommen von Smaragd, Alexandrit, Rubin und Saphir in einem Topas-fuehrenden Phlogopit-Fels von Poona, Cue District, West-Australien. Zeitschrift der Deutschen Gemmologischen Gesellschaft 44, 11–29.
Gübelin, E.J., 1958. Emeralds from Sandawana. Journal of Gemmology 6, 340–354.
Hammarstrom, J.M., 1989. Mineral chemistry of emeralds and some minerals from Pakistan and Afghanistan: an electron microprobe study. In: Kazmi, A.H., Snee, L.W. (Eds.), Emeralds of Pakistan. Van Nostrand Reinhold, New York, pp. 125–150.
Hanni, H.A., Klein, H.H., 1982. Ein Smaragdvorkommen in Madagaskar. Zeitschrift der Deutschen Gemmologischen Gesellschaft 21, 71–77.
Harrell, J.A., 2004. Archaeological geology of the world's first emerald mine. Geoscience Canada 31, 69–76.
Hickman, A.C.J., 1972. The Miku emerald deposit. Geological Survey of Zambia, Economic Report, vol. 27. 35 pp.
Hochleitner, R., 2002. Emerald: mineralogically a beryl. ExtraLapis 2, 10–17.
Jennings, R.H., Kammerling, R.C., Kovaltchouk, A., Calederon, G.P., El Baz, M.K., Koivula, J.I., 1993. Emeralds and green beryls of upper Egypt. Gems and Gemology 29, 100–115.
John, T., Schenk, V., Mezger, K., Tembo, F., 2004. Timing and PT evolution of whiteschist metamorphism in the Lufilian Arc-Zambezi Belt Orogen (Zambia): implications for the assembly of Gondwana. Journal of Geology 112, 71–90.
Just, E., 1926. Emeralds at Bom Jesus dos Meiras, Bahia. Economic Geology 21, 808–810.
Kanis, J., Schwarz, D., 2002. Emeralds of the world: Africa. ExtraLapis English 2, 52–59.
Kanis, J., Arps, C.E.S., Zwann, P.C., 1991. 'Machingwe': a new emerald deposit in Zimbabwe. Journal of Gemmology 22, 264–272.
Kazmi, A.H., Snee, L.W., 1989. Geology of the world emerald deposits: a brief review. In: Kazmi, A.H., Snee, L.W. (Eds.), Emeralds of Pakistan. Van Nostrand Reinhold, New York, pp. 165–228.
Kazmi, A.H., Lawrence, R.D., Anwar, J., Snee, L.W., Hussain, S., 1986. Mingora emerald deposits (Pakistan): suture-associated gem mineralization. Economic Geology 81, 2022–2028.
Keith, J.D., Thompson, T.J., Ivers, S., 1996. The Uinta emerald and the emerald-bearing potential of the Red Pine shale, Uinta Mountains, Utah. Geological Society of America, Abstracts with Programs 28, 85.
Keith, J.D., Nelson, S.T., Thompson, T.J., Dorais, M.J., Olcott, J., Duerichen, E., Constenius, K.N., 2002. The genesis of fibrous calcite and shale-hosted emerald in a non-magmatic hydrothermal system, Uinta mountains, Utah. Geological Society of America, Abstracts with Programs 34, 55.
Kovaloff, P., 1928. Geologist's report on Somerset emeralds. South African Mining and Engineering Journal 39, 101–103.
Kozlowski, A., Metz, P., Estrada Jaramillo, H.A., 1988. Emeralds from Somondoco, Colombia: chemical composition, fluid inclusions and origin. Neues Jahrbuch für Mineralogie. Abhandlungen 159, 23–49.
Kupriyanova, I.I., 2002. On the genesis of the Malyshevsk beryllium-emerald deposit (Middle Urals, Russia). Geology of Ore Deposits 44, 276–290.
Laskovenkov, A.F., Zhernakov, V.I., 1995. An update on the Ural emerald mines. Gems and Gemology 31, 106–113.
Laurs, B.M., Dilles, J.H., Snee, L.W., 1996. Emerald mineralization and metasomatism of amphibolite, Khaltaro granitic pegmatite hydrothermal vein system, Haramosh mountains, northern Pakistan. Canadian Mineralogist 34, 1253–1286.
Leitmeier, H., 1937. Das Smaragdvorkommen in Habachtal in Salzburg und seine Mineralien. Tschermak's Mineralogische und Petrographische Mitteilungen 49, 245–368.
Lewis, L.L., Hart, C.J.R., Murphy, D.C., 2003. Roll out the beryl. Yukon Geoscience Forum 2003.
Marshall, D., Groat, L., Giuliani, G., Murphy, D., Mattey, D., Ercit, T.S., Wise, M.A., Wengzynowski, W., Eaton, D.W., 2003. Pressure, temperature and fluid inclusion conditions during emerald precipitation, southeastern Yukon, Canada: fluid inclusion and stable isotope evidence. Chemical Geology 194, 187–199.
Marshall, D.D., Groat, L.A., Falck, H., Douglas, H., Giuliani, G., 2004. Fluid inclusions from the Lened emerald occurrence; Northwest Territories, Canada: implications for Northern Cordilleran Emeralds. Canadian Mineralogist 42, 1523–1539.
Martelat, J.-E., Lardeaux, J.-M., Nicollet, C., Rakotondrazafy, R., 2002. Strain pattern and late Precambrian deformation history in southern Madagascar. Precambrian Research 102, 1–20.
Martin, H.J., 1962. Some observations on southern Rhodesian emeralds and chrysoberyls. Journal of the Chamber of Mines 4, 34–38.
Martin-Izard, A., Moreiras, D., Acevedo, R.D., Paniagua, A., Marcos-Pascual, C., 1992. Génsis y medio de formación del yacimiento de minerales de berilo asociados a la pegmatita de Franqueira, Pontevedra (Galicia). Boletin Sociedad Española de Mineralogia 15, 216–221.
Martin-Izard, A., Paniagua, A., Moreiras, D., Acevedo, R.D., Marcos-Pascual, C., 1995. Metasomatism at a granitic pegmatite-dunite contact in Galicia; the Franqueira occurrence of chrysoberyl (alexandrite), emerald, and phenakite. Canadian Mineralogist 33, 775–792.
Martin-Izard, A., Paniagua, A., Moreiras, D., Acevedo, R.D., Marcos-Pascual, C., 1996. Metasomatism at a granitic pegmatite-dunite contact in Galicia; the Franqueira occurrence of chrysoberyl (alexandrite), emerald, and phenakite: Reply. Canadian Mineralogist 34, 1332–1336.
McManus, C.E., De Lucia, F., Harmon, R., McMillan, N.J., Whitmore, R., 2004. Trace element concentrations of pegmatite gems: tracers of petrogenesis and terrorist funding. Geological Society of America, Abstracts with Programs 36, 226.
Moine, B., Chan Peng, C., Mercier, A., 2004. Rôle du fluor dans la formation des gisements d'émeraude de Mananjary (Est de Madagascar). Comptes Rendus Geoscience 336, 513–522.
Moroz, I., Vapnik, Y., 1999. Fluid inclusions in emeralds from schist-type deposits. Canadian Gemmologist 20, 8–14.
Moroz, I., Vapnik, Y., Eliezri, I., Roth, M., 2001. Mineral and fluid inclusion study of emeralds from the Lake Manyara and Sumbawanga deposits. Journal of African Earth Sciences 33, 377–390.

Mumme, I., 1982. The Emerald, Its Occurrence, Discrimination and Valuation. Mumme Publications, New South Wales. 135 pp.
Murphy, D.C., Lipovsky, P.S., Stuart, A., Fonseca, A., Piercey, S.J., Groat, L., 2002. What about those emeralds, eh? Geological setting of emeralds at Regal Ridge (SE Yukon) provides clues to their origin and to other places to explore. Geological Association of Canada, Mineralogical Association of Canada, Abstracts with Programs 28, 154.
Nassau, K., 1983. The Physics and Chemistry of Color: The Fifteen Causes of Color. John Wiley and Sons, New York. 480 pp.
Neufeld, H.L.D., 2004. The Tsa da Glisza Emerald Occurrence, Finlayson Lake District, Southeastern Yukon Territory, Canada: Descriptive, Genetic, and Exploration Models. Unpublished M.Sc. thesis, University of British Columbia, Vancouver, BC, Canada, 108 pp.
Neufeld, H.L.D., Groat, L.A., Mortensen, J.K., 2003. Preliminary investigations of emerald mineralization in the Regal Ridge area, Finlayson Lake district, southeastern Yukon. In: Emond, D.S., Lewis, L.L. (Eds.), Yukon exploration and geology 2002.Exploration and Geological Services Division, Yukon Region, Indian and Northern A airs Canada, pp. 281–284.
Neufeld, H.L.D., Israel, S., Groat, L.A., Mortensen, J.K., 2004. Geology and structural setting of the Regal Ridge emerald property, Finlayson Lake district, southeastern Yukon. In: Emond, D.S., Lewis, L.L. (Eds.), Yukon Exploration and Geology 2003. Yukon Geological Survey, pp. 281–288.
Nwe, Y.Y., Grundmann, G., 1990. Evolution of metamorphic fluids in shear zones: the record from the emeralds of Habachtal, Tauern window, Austria. Lithos 25, 281–304.
Nwe, Y.Y., Morteani, G., 1993. Fluid evolution in the H_2O–CH_4–CO_2–NaCl system during emerald mineralization at Gravelotte, Murchinson greenstone belt, Northeast Transvaal, South Africa. Geochimica et Cosmochimica Acta 57, 89–103.
Ohnenstetter, D., Giuliani, G., Bustos, O., 1998. Emeraudes trapiches colombiennes. In: Giard, D., Giuliani, G., Cheilletz, A., Fritsch, E., Gonthier, E. (Eds.), L'Émeraude, Connaissances Actuelles et Prospectives. Association Française de Gemmologie, Paris, pp. 119–124.
Olcott, J.D., Duerichen, E., Nelson, S.T., Keith, J.D., Tingey, D.G., 1998. Genesis of economic fibrous calcite veins, Uinta Mountains, Utah. Geological Society of America, Abstracts with Programs vol. 30, 371.
Otero Muñoz, G., Barriga Villalba, A.M., 1948. Esmeraldas de Colombia. Banco de la Republica, Bogota.
Ottaway, T.L., 1991. The Geochemistry of the Muzo Emerald Deposit, Colombia. Unpublished M.Sc. thesis, University of Toronto, Toronto, ON, Canada, 216 pp.
Ottaway, T.L., Wicks, F.J., Bryndzia, L.T., Keyser, T.K., Spooner, E.T.C., 1994. Formation of the Muzo hydrothermal emerald deposit in Colombia. Nature 369, 552–554.
Panjikar, J., Ramchandran, K.T., Balu, K., 1997. New emerald deposits from southern India. Australian Gemmologist 19, 427–432.
Petrusenko, S., Arnaudov, V., Kostov, I., 1966. Emerald pegmatite from the Urdini Lakes, Rila Mountains. Annuaire de l'Université de Sofia, Faculté de Géologie et Géographie 59, 247–268.
Renders, P.J., Anderson, G.M., 1986. Solubility of kaolinite and beryl to 573 K. Applied Geochemistry 2, 193–203.
Ringsrud, R., 1986. The Coscuez mine: a major source of Colombian emeralds. Gems and Gemology 22, 67–79.
Robb, L.J., Robb, V.M., 1986. Archean pegmatite deposits in the northeastern Transvaal. In: Anhaeusser, C.R., Maske, S. (Eds.), Mineral Deposits of Southern Africa. Geological Society of South Africa, vol. 1, pp. 437–450.
Rudnick, R.L., Gao, S., 2003. The composition of the continental crust. In: Rudnick, R.L. (Ed.), The Crust. Treatise on Geochemistry, vol. 3, pp. 1–64.
Sabot, B., 2002. Classification des gisements d'emeraude: apports des etudes petrographiques, mineralogiques et geochimiques. Unpublished Ph.D. thesis, Institut National Polytechnique de Lorraine, France. Vol. 1, 172 pp.
Sabot, B., Cheilletz, A., de Donato, P., Banks, D., Levresse, G., Barrès, O., 2000. Afghan emeralds face Colombian cousins. Chronique de la Recherche Minière 541, 111–114.
Sabot, B., Cheilletz, A., de Donato, P., Banks, D., Levresse, G., Barrès, O., 2002. The Panjshir-Afghanistan emerald deposit: new field and geochemical evidence for Colombian style mineralisation, vol. 548. European Union of Geosciences. Abstracts.
Schultz-Güttler, R.A., Romero-Ordonez, F.H., 2000. Rb/Sr geochemistry and the age of the Colombian emerald mineralization. 29th International Geological Congress, Abstracts CD-ROM, vol. 31.
Schwarz, D., 1991. Australian emeralds. Australian Gemmologist 17, 488–497.
Schwarz, D., Giuliani, G., 2001. Emerald deposits — a review. Australian Gemmologist 21, 17–23.
Schwarz, D., Giuliani, G., 2002a. South America: Colombia. ExtraLapis English 2, 36–45.
Schwarz, D., Giuliani, G., 2002b. South America: Brazil. ExtraLapis English 2, 46–51.
Schwarz, D., Giuliani, G., 2002c. Emeralds from Asia. ExtraLapis English 2, 60–63.
Schwarz, D., Schmetzer, K., 2002. The definition of emerald. ExtraLapis English 2, 74–78.
Schwarz, D., Kanis, J., Kinnaird, J., 1996. Emerald and green beryl from central Nigeria. Journal of Gemmology 25, 117–141.
Schwarz, D., Giuliani, G., Grundmann, G., Glas, M., 2001. Die Entstehung der Smaragde, ein vieldisskutiertes Thema. In: Schwarz, D., Hochlitner, R. (Eds.), Smaragd, der kostbarste Beryll, der teuerste Edelstein. ExtraLapis, vol. 21, pp. 68–73.
Schwarz, D., Giuliani, G., Grundmann, G., Glas, M., 2002. The origin of emerald...a controversial topic. ExtraLapis English 2, 18–21.
Seal II, R.R., 1989. A reconnaissance study of the fluid inclusion geochemistry of the emerald deposits of Pakistan and Afghanistan. In: Kazmi, A.H., Snee, L.W. (Eds.), Emeralds of Pakistan. Van Nostrand Reinhold, New York, pp. 151–164.
Seifert, A.V., Žáček, V., Vrána, S., Pecina, V., Zachariáš, J., Zwaan, J.C., 2004. Emerald Mineralization in the Kafubu area, Zambia. Bulletin of Geosciences 79, 1–40.
Sheppard, S.M.F., 1986. Characterisation and isotopic variations in natural waters. In: Valley, J.W., TaylorJr. Jr., H.P., O'Neil, J.R. (Eds.), Stable Isotopes in High Temperature Geological Processes. Reviews in Mineralogy, vol. 16, pp. 165–183.
Simandl, G.J., Paradis, S., Birkett, T., 1999a. Schist-hosted emeralds. In: Simandl, G.J., Hora, Z.D., Lefebure, D.V. (Eds.), Selected British Columbia Mineral Deposit Profiles. . Industrial Minerals, vol. 3. British Columbia Ministry of Energy and Mines. Open File 1999–10, 137 pp.
Simandl, G.J., Paradis, S., Birkett, T., 1999b. Colombia-type emeralds. In: Simandl, G.J., Hora, Z.D., Lefebure, D.V. (Eds.), Selected British Columbia Mineral Deposit Profiles. . Industrial Minerals, vol. 3. British Columbia Ministry of Energy and Mines. Open File 1999–10, 137 pp.
Simpson, E.S., 1948. Minerals of Western Australia. Perth Government Printer 1, 195–207.
Sunagawa, I., 2005. Crystals-Growth, Morphology and Perfection. Cambridge University Press, Cambridge, UK. 295 pp.
Surour, A.A., Takla, M.A., Omar, S.A., 2002. EPR spectra and age determination of beryl from the Eastern Desert of Egypt. Annals of the Geological Survey of Egypt 25, 389–400.
Tappen, C.M., 1998. Beryl and Tourmaline Mineralization of the Crabtree Pegmatite, Spruce Pine District, North Carolina. Unpublished M.Sc. thesis, University of North Carolina, Wilmington, NC, 115 pp.
Taylor, R.P., Fallick, A.E., Breaks, F.W., 1992. Volatile evolution in Archean rare-element granitic pegmatites: evidence from the hydrogen-isotopic composition of channel H_2O in beryl. Canadian Mineralogist 30, 877–893.
Themelis, T., 1989. Gemmology; new east African deposits. Lapidary Journal 42, 34–37.
Torres, I.E., 2001. The mineral industry of Colombia. United States Geological Survey Minerals Yearbook (http://minerals.usgs.gov/minerals/pubs/country/2001/comyb01r.pdf).
Vapnik, Ye., Moroz, I., 2000. Fluid inclusions in emerald from the Jos Complex (central Nigeria). Schweizerische Mineralogische und Petrographische Mitteilungen 80, 117–129.
Vapnik, Ye., Moroz, I., 2001. Fluid inclusions in Panjshir emerald (Afghanistan). Proceedings of the XVI European current research on fluid inclusions (ECROFI), pp. 451–454.
Vapnik, Ye., Moroz, I., 2002. Compositions and formation conditions of fluid inclusions in emerald from the Maria deposit (Mozambique). Mineralogical Magazine 66, 201–213.
Vapnik, Ye., Sabot, B., Moroz, I., 2005. Fluid inclusions in Ianapera emerald, Southern Madagascar. International Geology Review 47, 647–662.
Vapnik, Ye., Moroz, I., Eliezri, I., 2006. Formation of emeralds at pegmatite-ultramafic contacts based on fluid inclusions in Kianjavato emerald, Mananjary deposits, Madagascar. Mineralogical Magazine 70, 141–158.
Vinogradova, E.A., 1996. Determination of main objects for precious stones prospecting in the Republic of Kazakhstan, with the selection of areas for special geological-mineralogical mapping on a scale of 1:200,000. Report of the works from the period 1995–96. Archives of the Ministry of Geology of Kazakhstan Republic, Mirniy.
Vlasov, K.A., Kutakova, E.I., 1960. Izumrudnye Kopi. Moscow Akademiya Nauk SSGR. 252 pp.
Walton, L., 2004. Exploration Criteria for colored Gemstone Deposits in the Yukon. Yukon Geological Survey, Open File 2004-10. 184 pp.
Ward, F., 2001. Emeralds. Gem Book Publishers, Bethesda, MD. 64 pp.
Wise, M.A., 2002. New finds in North Carolina. ExtraLapis English 2, 64–65.
Wise, M.A., Anderson, A.J., 2006. The emerald- and spodumene-bearing quartz veins of the Rist emerald mine, Hiddenite, North Carolina. Canadian Mineralogist 44, 1529–1541.
Zachariáš, J., Žáček, V., Pudilová, M., Machovič, V., 2005. Fluid inclusions and stable isotope study of quartz-tourmaline veins associated with beryl and emerald mineralization, Kafubu area, Zambia. Chemical Geology 223, 136–152.
Zachovay, M., 2002. What is the price of an emerald? ExtraLapis English 2, 93–96.
Zambonini, F., Caglioto, V., 1928. Ricerche chimiche sulla rosterite di San Piero in Campo (Isola d'Elba) e sui berilli in generale. Gazzetta Chimica Italiana 58, 131–152.
Zhang, S., Feng, M., Lu, W., 1998. Analysis of the Nanwenhe metamorphic core complex in southeastern Yunnan. Regional Geology of China 17, 390–397.
Zhang, S., Feng, M., Wang, H., Lu, W., 1999. Geological features and genesis of emerald deposit in Malipo County, Yunnan, China. Geological Science and Technology Information 18, 50–54.
Zwaan, J.C., 2006. Gemmology, geology and origin of the Sandawana emerald deposits, Zimbabwe. Scripta Geologica 131 211 pp.
Zwaan, J.C., Kanis, J., Petsch, E.J., 1997. Update on emeralds from the Sandawana mines, Zimbabwe. Gems and Gemology 33, 80–100.
Zwaan, J.C., Seifert, A., Vrána, S., Laurs, B.M., Anckar, B., Simmons, W.B., Falster, A.U., Lustenhouwer, W.J., Muhlmeister, S., Koivula, J.I., Garcia-Guillerminet, H., 2005. Emeralds from the Kafubu area, Zambia. Gems and Gemology 41, 116–148.